UNIVERSIDADE D
COIMBRA

Francisco Rafael dos Reis Cruz

PROCESSOS ADITIVOS E COBRE

Dissertação no âmbito do Mestrado Integrado em Engenharia Mecânica, na especialidade de Produção e Projeto, orientada pela Professora Doutora Maria Teresa Freire Vieira e pelo MSc Daniel Alexandre Cruz Gatões e apresentada ao Departamento de Engenharia Mecânica da Faculdade de Ciências e Tecnologias da Universidade de Coimbra

Julho de 2019

FACULDADE DE CIÊNCIAS E TECNOLOGIA
UNIVERSIDADE D COIMBRA

Additive Manufacturing and Copper

Submitted in Partial Fulfilment of the Requirements for the Degree of Master in Mechanical Engineering in the speciality of Production and Project

Processos Aditivos e Cobre

Author

Francisco Rafael dos Reis Cruz

Advisors

Maria Teresa Freire Vieira

Daniel Alexandre Cruz Gatões

Jury

President	**Doutora Ana Sofia Figueira Ramos** **Investigadora DL57 da Universidade de Coimbra**
Vowel	**Professora Doutora Fátima Maria Carvalhinhas Barreiros** **Professora Coordenadora do Instituto Politécnico de Leiria**
Advisor	**Professora Doutora Maria Teresa Freire Vieira** **Professora Catedrática da Universidade de Coimbra**

Coimbra, July, 2019

Whether you think you can or think you can’t, you’re right.

Henry Ford

ACKNOWLEDGEMENTS

I thank Professora Doutora Teresa Vieira, for providing me with the opportunity to participate in this research project, for believing in my capabilities, for being patient and for all the knowledge and teachings she transmitted me, for which I am meaningfully grateful.

I thank Daniel Gatões, for his vital contribution and guidance. He was a true mentor, lighting the way when the path was not clear. Without his dedication and continuous support, writing this thesis would not have been possible.

I thank Fábio for all he taught me about filament fabrication and for his availability.

I thank my laboratory colleagues for the relaxing moments, especially to Renata and Hugo for their help with the feedstock mixtures.

I thank IPN/LED & MAT group for always keeping the door open for me and being welcoming.

I thank Magda, for backing me up in the hard times and inspiring me to keep going forward.

I thank my brother Pedro, for all the incentive, support and care, in both fair winds and storms. I feel blessed for having him as part of my life.

I thank my parents, Ângela and Nelson, for unconditionally supporting and encouraging me throughout the hole of my studies and life. Their affect and dedication are the foundations of everything I have achieved.

Abstract

In this century, consumer needs are becoming increasingly challenging. The industry 4.0 is revolutionising both production and delivering sectors, blurring the lines between physical and digital. With the possibility of custom-made products, new ideas will flourish with geometries that could not be made until now. In this paradigm, Additive Manufacturing appears as a fundamental pillar sustaining this technological trend. It comprises different step-by-step technologies that often utilise powders to produce the final parts/systems.

Selective Laser Melting is the most common printing process. However, regarding the mould industry, this technology cannot be used alone to obtain near net shape parts. Another problem is the interaction between the laser and powder, which assumes great importance in the case of copper. This powder has other drawbacks, high thermal conductivity and reflectivity, that contribute to increase defects inside and in the surface of additive parts/systems.

If possible, applying Fused Deposition Modelling (FDM) technology to manufacturing copper powders based on the PIM methodology could be the solution. A polymeric filament-extrusion based technique was used to produce parts/systems by FDM, that assumes in this case the designation of FDMet.

The present study shows that it is possible, with great success, to produce copper inserts of moulds with complex geometries by FDMet, with constructal cooling channels, from filaments made by metallic powder extrusion. The feedstocks were optimized by mixing copper powder with different polymers, each one with a specific function. After filament extrusion for part/system building, debinding and sintering processes, typical of conventional copper powder technology, was performed.

Keywords Additive Manufacturing (AM), Fused Deposition of Metals (FDMet), Filament, Inserts, Constructal cooling channels, Copper powder.

Resumo

Neste século, as necessidades dos consumidores são cada vez mais desafiantes. A indústria 4.0 está a revolucionar ambos os sectores de entrega e produção, eliminando a separação entre o digital e o físico. Perante a possibilidade de criar produtos personalizados, novas ideias irão florescer com geometrias que até agora não podiam ser concretizadas. Neste paradigma, o Fabrico Aditivo surge como um pilar fundamental que sustenta esta tendência tecnológica. Abrange diferentes tecnologias de passo-a-passo que frequentemente utilizam pós para produzir produtos finais.

O processo de impressão mais frequentemente utilizado é a Fusão Seletiva por Laser. No entanto, no que toca à indústria de moldes, esta técnica não pode ser usada isoladamente para obtenção de peças finais. Outra problemática é a interação entre laser e pó, de grande importância no caso do cobre. Outras desvantagens deste pó são as elevadas condutividade térmica e refletividade, que contribuem para aumentar os defeitos no interior e à superfície das partes ou sistemas aditivos.

Se possível, aplicar a tecnologia de Modelagem por Deposição Fundida (FDM) à manufatura de pós de cobre baseada em metodologia PIM poderá ser a solução. Foi usada uma técnica baseada na extrusão de filamento polimérico para produzir partes ou sistemas por FDM, que neste caso assume a designação de FDMet.

Este estudo demonstra que é possível, com grande sucesso, produzir insertos de cobre de moldes com elevada complexidade geométrica por FDMet, com canais de arrefecimento constructais, a partir de filamentos criados por extrusão de pó metálico. Os *feedstocks* foram otimizados ao misturar pó de cobre com diferentes polímeros, cada um com uma função específica. Após a extrusão de filamento para a construção de partes/sistemas, foram realizados os processos de eliminação do ligante e de sinterização típicos de tecnologia de pó de cobre convencional.

Palavras-chave: Fabrico Aditivo, Deposição Fundida de Metais (FDMet), Filamento, Insertos, Canais de refrigeração contructais, Pó de cobre.

Contents

LIST OF FIGURES

LIST OF TABLES

LIST OF SYMBOLS, ACRONYMS AND ABBREVIATIONS

List of Symbols

α – Secondary channels return flow angle (or divergence angle)

θ – Angle of diffraction (scattering angle)

λ – Wavelength of the incident wave

ρ – Density

d_{10} – Particle diameter which is greater than 10 % of the distribution

d_{50} – Median particle size

d_{90} – Particle diameter which is greater than 90 % of the distribution

D_i – Channel diameter

d_p – Interplanar distance between lattice planes

E – Young modulus

L_i – Channel length

M1 – Commercial Binder

n – Number of secondary channels

n_b – Diffraction order (positive integer)

Ra – Arithmetical mean deviation of roughness profile

Rq – Root mean squared of roughness profile

Rz – Roughness profile based on the five highest peaks and lowest valleys over the entire sampling length

Sv – Sveltness

S_w – Particle size distribution width

Vol. % – Volume percentage

Y_{av} – Average yield stress

Acronyms and Abbreviations

3D – Three-dimensional

AM – Additive Manufacturing

CAD – Computer-aided Design

CPVC – Critical Powder Volume Concentration

FDM™ – Fused Deposition Modelling

FDMet – Fused Deposition of Metals

FVM/IFM – Focus Variation Microscopy/Infinite Focus Microscopy

HIP – Hot Isostatic Pressure

ISO – International Organization for Standardization

IUPAC – International Union of Pure and Applied Chemistry

LDS – Laser Diffraction Spectrometry

OM – Optical Microscopy

PIM – Powder Injection Moulding

PSD – Particle Size Distribution

SA – Stearic Acid

SEBS – Styrene and Ethylene/Butylene

SEM – Scanning Electron Microscopy

SLM – Selective Laser Melting

STL – Standard Tessellation Language (or Standard Triangle Language)

TGA – Thermogravimetric Analysis

TPE – Thermoplastic Elastomer

XRD – X-rays Diffraction

INTRODUCTION

Additive Manufacturing (AM) is the general designation for technologies that create physical objects by successive addition of material based on a geometrical representation, according to the International Organization for Standardization (ISO) [1]. These technologies, also known as 3D Printing, are open source collaboration and intelligent technologies, and are considered the key driver behind the ongoing paradigm shift of the 21st century post-industrial order [2]. Nowadays the demanding exclusive, efficient, cheap and eco-friendly products are met by AM. 3D Printing has been demonstrated to improve product performance, reduce work times, eliminate the need for tooling and allow the creation of parts with complex geometries which would otherwise be impossible to produce with conventional manufacturing [3].

Despite its potential, AM of metal powders is not yet a widespread adopted method for core production. This could be due to various aspects [4]:

- size limitation;
- quality consistency;
- scalability limitations;
- narrow range of eligible materials and high material cost;
- and limited multimaterial capabilities.

Selective Laser Melting (SLM) stands out as the most commonly AM used for the production of parts/systems from metallic powders. Moreover, it produces fully dense objects with properties similar to bulk materials. However, some metallic materials (like copper) are not appropriate for SLM, due to their laser absorption, thermal conductivity, surface tension and/or viscosity [5]–[7].

With the impossibility of producing high quality copper components through SLM [8], the window of opportunity is now open for Fused Deposition of Metals (FDMet) to stand out in the AM industry. FDMet is a technology for processing metals derived from Fused Deposition Modelling (FDM™), a polymeric filament-based technique. In opposition to SLM, FDMet appears as a low-cost solution for the copper powder [9].

The aim of this dissertation is to produce mould copper inserts with and without cooling channels, following the constructal theory, from feedstock mixtures, through FDMet (shaping) to debinding and sintering (consolidation), supported by Powder Injection Moulding (PIM) methodology.

Different steps must be done to achieve this objective, as follows:

- material selection;
- feedstocks production;
- filament extrusion;
- 3D shaping;
- debinding and sintering.

This thesis is constituted by Introduction, Chapters 1 to 3, Conclusion and annotations for Future Work. Chapter 1 presents a description of the state of art regarding AM, copper properties, FDMet equipment and process, debinding, sintering and the constructal principle. Chapter 2 describes the materials and equipment required to produce and characterise the parts, namely binder and feedstock, as well as the methods and techniques used, like feedstock mixing, 3D printing, gas pycnometry, laser diffraction spectroscopy, X-rays diffraction, optical microscopy, scanning electron microscopy and focus variation microscopy. Chapter 3 states the results and their analysis having in mind the current bibliography, regarding the powder characterization, filament manufacturing, FDMet procedure, debinding, sintering and FDMet parts characterization.

1. STATE OF ART

The fourth industrial revolution is changing the world and its manufacturing. Instead of standardised mass production, the emphasis is now shifting towards custom-made, individually adapted components of high quality and low cost [10], [11]. This paradigm shift has led to high market competition, as numerous companies try to improve production techniques while reducing costs.

Additive Manufacturing (AM) is a promising solution for such a demand [11]. It consists in binding material in order to produce components following a 3D Computer-aided Design (CAD) model, usually in a layer-by-layer method. Thus, it is capable of creating small and complex parts without the extra costs of precision detailing of subtractive methodologies.

AM has many applications and advantages. For example, by sending a digital 3D object file, it is possible to print a component of polymer, metal or ceramic on-site, avoiding transportation costs and time. It is one of the fastest growing fabrication technologies in the world [12], with a highly competitive market embracing many fields, from commerce of printers to powder production.

As a consequence of such competition, AM research has been hampered by patents. Studies concerning metallic powder sintering date back to the 1940s [13]. In 1989, Stratasys is founded by S. Scott Crump after he patented a method which would later become Fused Deposition Modelling (FDM™) [14]. After it expired in 2009, the number of research publications regarding AM began to increase exponentially (Figure 1)

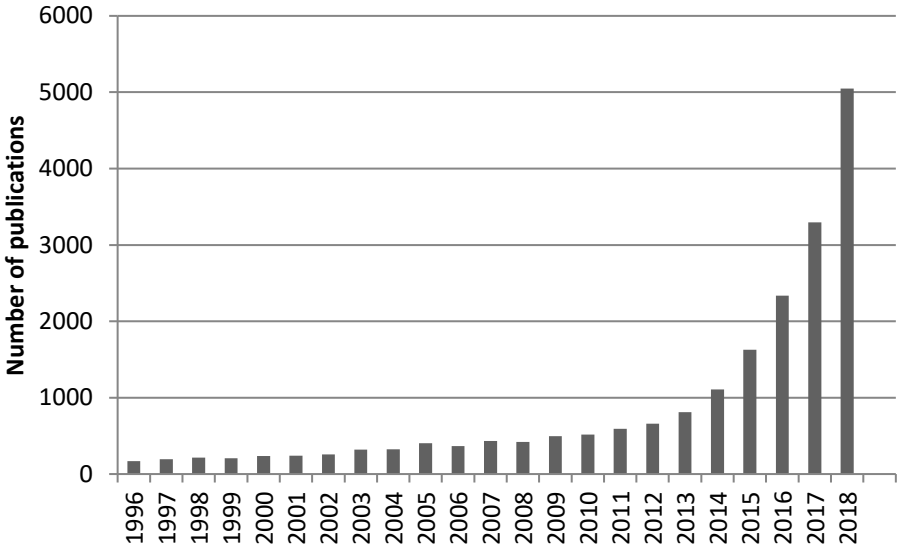

Figure 1 - Number of publications concerning AM. Number of review articles, research articles, case reports, data articles, mini reviews on ScienceDirect© database with the keyword(s) fused filament fabrication, fused deposition modelling, filament freeform

The objectives that AM research pursuits can be summarised as the "3 Fs": Form, Fit and Function. Form was the initial challenge, essentially consisting on enabling the creation of objects of a desired shape. After the first parts were produced, other needs soon became clear: to manufacture components with high-quality surface finishing not requiring extensive post-treatments (Fit) and to create mechanically strong, load-bearing parts (Function) [15], [16].

Regarding the latter, using metals in AM became an area of great interest. It would allow the creation of mechanically robust but very small and lightweight components, in line with contemporary engineering trends [12], [17]. However, certain challenges remain unanswered, such as developing AM technologies capable of using copper powders.

1.1.1. Copper

Pure copper at atmospheric conditions is a soft, ductile, corrosion resistant metal with very high thermal conductivity and exceptional electrical conductivity (Table 1) [18], [19]. It also has other characteristics not directly related to this study purpose, such as having good biofouling resistance and machinability, high retention of mechanical and electrical properties at cryogenic temperatures and being a non-magnetic material [20].

Table 1 - Properties of copper

Property	Copper value	Reference
Melting temperature [ºC]	1083	[18]
Young modulus (*E*) [GPa]	36	[18]
Poisson ratio (*v*)	0.34	[18]
Thermal conductivity (at 20ºC) [W/mK]	40	[18], [19]
Specific heat (at 20ºC) [J/kgK]	386	[19]
Density (ρ) [kg/m^3]	8960	[19]

Regarding its structure, copper has a face centred cubic (fcc) crystal structure. It is yellowish red in physical appearance and when polished develops a bright metallic lustre.

When sintering, it is necessary to take into account the decrease of the average yield stress (Y_{av}) of copper with temperature (Figure 2).

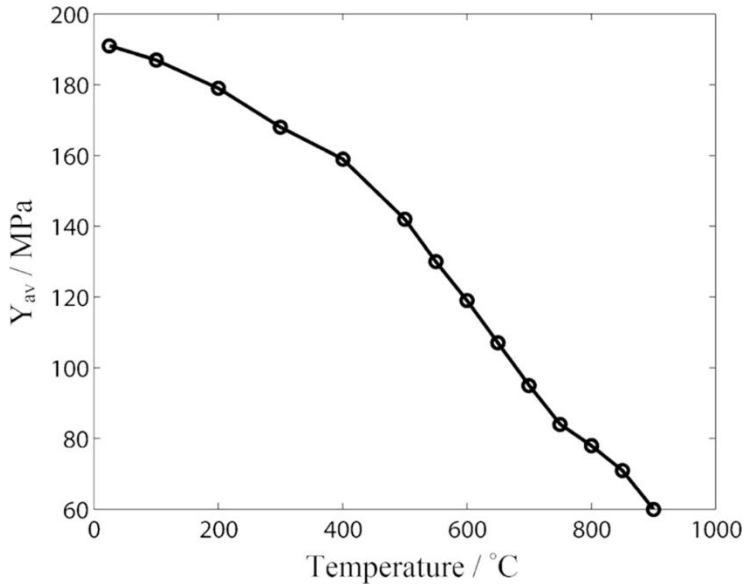

Figure 2 - Interpolation representing the average yield stress (MPa) versus temperature (°C) for pure copper (adapted from [21]**)**

Regarding the sintering atmosphere, it is necessary to know its gases solubility in copper. Nitrogen, argon and hydrogen are the eligible gases for the sintering atmosphere, but only hydrogen has a phase diagram (Figure 3), argon is an inert gas and nitrogen is not soluble in copper at the sintering temperature [22], [23].

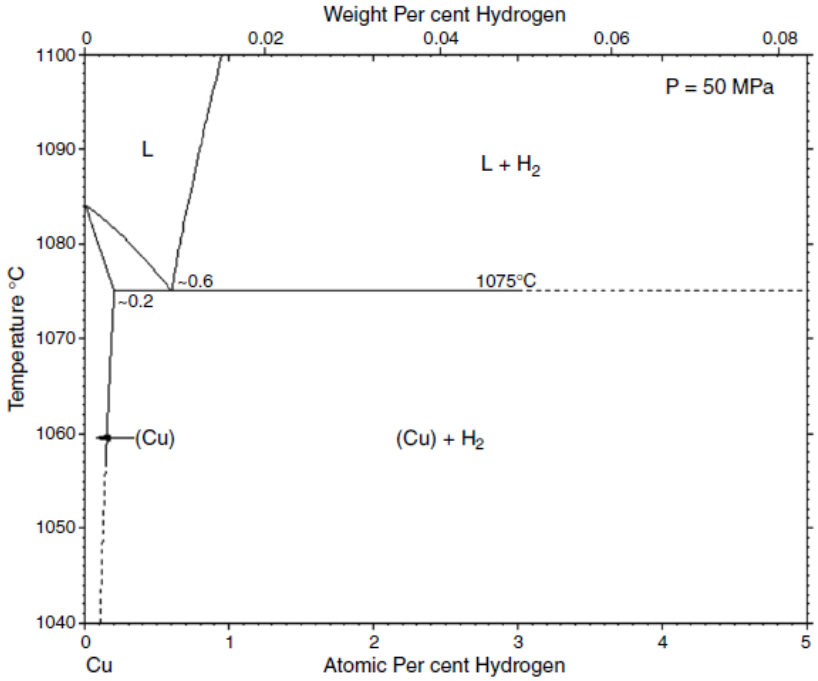

Figure 3 - Copper-hydrogen phase diagram (adapted from [24]**)**

Copper and copper alloy can also be used in an extraordinary range of applications besides the building industry such as power transmission lines, architectural applications, cooking utensils, spark plugs, electrical wiring, cables and busbars, high conductive wires, electrodes, heat exchangers, refrigeration tubing, plumbing or water-cooled copper crumbles.

1.1.2. FDMet Equipment

The 3D printer has a controller board, a filament, a frame, toothed belts, lead screws, stepper motors, end stops, a power supply unit, a print bed, a print bed surface, a print head and cooling fans.

The controller board directs the motion components, following computer commands and the sensors input. Its quality has a major impact on the printer performance.

The material which is used to print objects is the filament. Most 3D printers use filaments of diameter 1.75 mm [15], but diameters ranging from 1.70 to 1.80 mm ± 0.05 mm are considered acceptable [25].

The frame physically supports the other components. It should be made of metal to ensure maximum stability and durability [26]. According to its arrangement, the 3D

printer can be classified as Cartesian, with a simple XYZ arrangement, or Delta, with three arms which rotate all-around.

The motion components move the print bed and the print head in three axes. They include the toothed belts, lead screws and stepper motors. Any misalignment of the components has direct influence on the end products quality, originating visible printing errors.

The stepper motors, operated by the stepper drivers, rotate in increments or steps, which makes them better suited for 3D printers than regular DC motors. There is also a stepper motor feeding the extruder in the print head.

The toothed belts, in a Cartesian model, move the X and Y-axis and are crucial for printing speed and precision. A whole print can be compromised by a single loose belt, so many printers have belt tensioners. The Z-axis movement uses rotating lead screws to move the print head vertically.

The end stops can be mechanical or optical, and keep components from being damaged by movements beyond their appropriate range.

The filament is deposited on the print bed to form an object. The print bed can be heated, as it is required to diminish warping [26] in high-temperature filaments. On the print bed there is the print bed surface or build surface, which adheres to the part being printed and facilitates its removal.

The print bed can be made of steel, aluminium or glass. To improve adhesion, an adhesive tape with acrylonitrile butadiene styrene (ABS) poured on it can be added to the print bed surface.

The print head, also known as the extruder, prints the filament into the 3D part. In its cold end, the filament drive gear forces the filament down into the hot end, where the filament is melted by the heater cartridge and poured by a nozzle. To keep the filament from melting before reaching the nozzle there are a heat sink and a heat sink fan, with a thermocouple or thermistor acting as temperature sensor.

The nozzle diameter has to be chosen according to the situation. Most printers have a 0.4 mm nozzle by default [15], but a smaller diameter renders higher print detail while a larger one allows for faster printing speeds. It is possible to easily change the nozzle during a printing session, in order to print high detail areas easier but ensure the necessary level of detail in the most complex zones of the part.

There is also a sensor on the print head which ensures its alignment with the build surface by scanning various points on the latter. The levelling itself is carried out by an automatic bed levelling system or by manually adjusting the thumbwheels, depending on the printer model.

Finally, just as the filament laid on the print bed, the cooling fans help it preserve its form, being programmed according to the type of filament.

1.1.3. FDMet Process

In FDMet, first, the 3D part Computer Aided Design (CAD) is created, analysed and optimised using a specific software. Alternatively, it can be obtained from 3D scanners, computed tomography scans or magnetic resonance imaging [27]. Next, the CAD is usually processed into a Standard Triangulation or Tessellation Language (STL) file, although other file types such as ASTM ISO Additive Manufacturing File Format (AMF) or other emerging file types [27]–[29]. Using a dedicated software, this file is then virtually cut in layers of the specified height and the print head and print bed movements are programmed together with other parameters, generating the G-Code [28].

To obtain non-commercial filament, the chosen materials are mixed and processed into the filament that will be used for printing, using a binder to carry the desired end product materials. The FDMet equipment then moves the print head in the three axes according to the G-Code, depositing the material at a constant rate in successive layers. The print head volumetric feed rate (cm^3/min) of filament should be equal to the nozzle volumetric flow rate (cm^3/min) of extruded filament, but in reality, there are always losses which can affect the filament flow, and should thus be assessed [30].

To obtain bulk metal parts, other processes are necessary. Debinding removes the binder from the green printed part, and sintering causes the remaining particles to adhere and consolidate. Sometimes, the printed part has supports, sections printed to help other sections hold their shape (for example, a column supporting an arc) that need to be removed, or it may be beneficial for the sintered part to undergo a post-treatment like Hot Isostatic Pressure (HIP), polishing or coating.

The FDMet process is represented in Figure 4

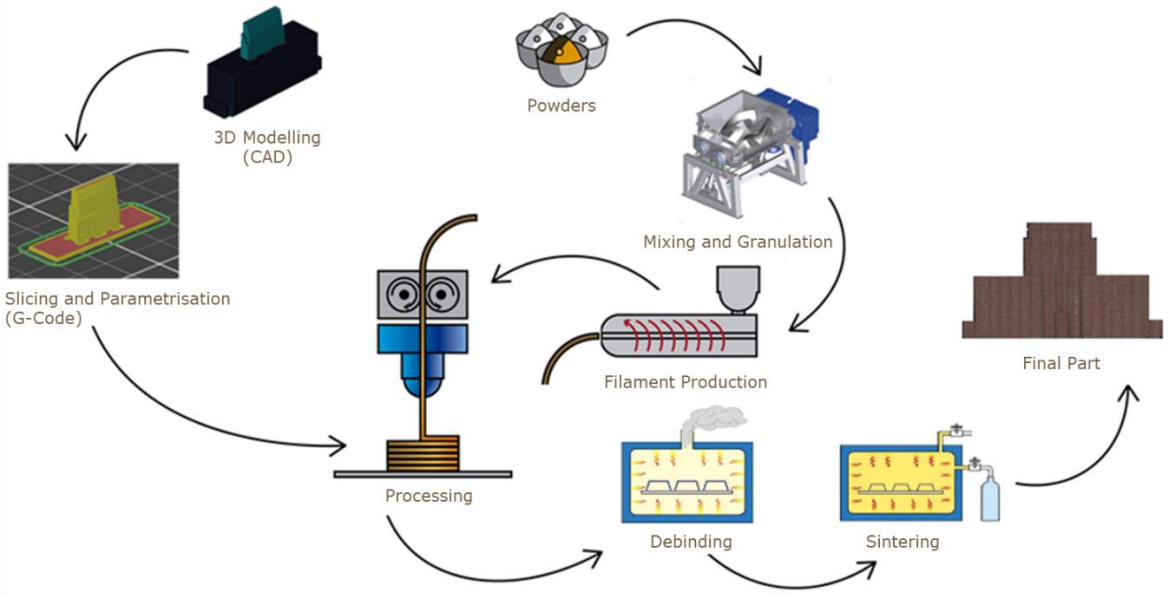

Figure 4 - FDMet process

The material extrusion method can be based on a plunger, screw or filament.

Desktop Metal Inc. and Markforged Inc. printers use the plunger technology, where a piston causes the flowing of the molten material. The screw approach uses a rotating screw to pump the material. This study used the filament technique, in which a filament of solid material is used to feed the print head, which will then melt it [15], [27], [31].

In order to feed the print head, the filament has to be pulled. Heating increases its malleability, so it is less likely to break. The filament is subjected to gravity and the forces applied by the extruder gear wheels, which result from the wheels momentum and cause small plastic deformities in the filament. These increase friction and allow the gear wheels forces to be applied more efficiently [15].

The extruder printing channel has annular fins which cool the filament. Further cooling comes from external fans pointing to the printing channel and printing zone.

The adhesion to the print bed surface is crucial for the integrity of the printing. It can be increased by cooling the printed filament and by applying certain printing techniques. These include skirts, brims and rafts. A skirt consists in discarding the initial portion of the filament, which is not yet fully heated, by printing it around the edge of the print surface with no contact with the following print sections. Creating an extra brim of material extending from the printed part first layer increases the contact area with the build surface and thus the adhesion, which helps preventing the part from detaching from the build surface. The part adhesion to the surface can be further enhanced by printing it onto a raft,

that is, a layer of filament with parallel ditches. Sometimes this uneven surface can cause the deposited filament to bend or even topple into the ditches.

As for the adhesion between different layers, it depends on the printing speed and layer height, which can be adjusted during the first layers but should remain unaltered for the rest of the process.

1.1.4. Debinding

Debinding consists in removing the polymeric binder leaving a porous structure, in both FDMet and PIM, and it must not disrupt the green part. It is the longest step and is among the most crucial phases of manufacturing [27] because leaving any carbon residue from the polymers can disturb sintering, generate vapours that cause defects such as blistering, bloating, surface cracking or internal voids if the vapours partial pressure surpasses atmospheric pressure [32], and thus impact on the end product.

The three main methods for debinding are the thermal, solvent, and catalytic techniques [33].

The thermal approach is the most commonly used (Figure 5). Heating the binder causes it to melt and flow out, or to thermally degrade and then diffuse out of the printed part. The temperature required depends on the binder.

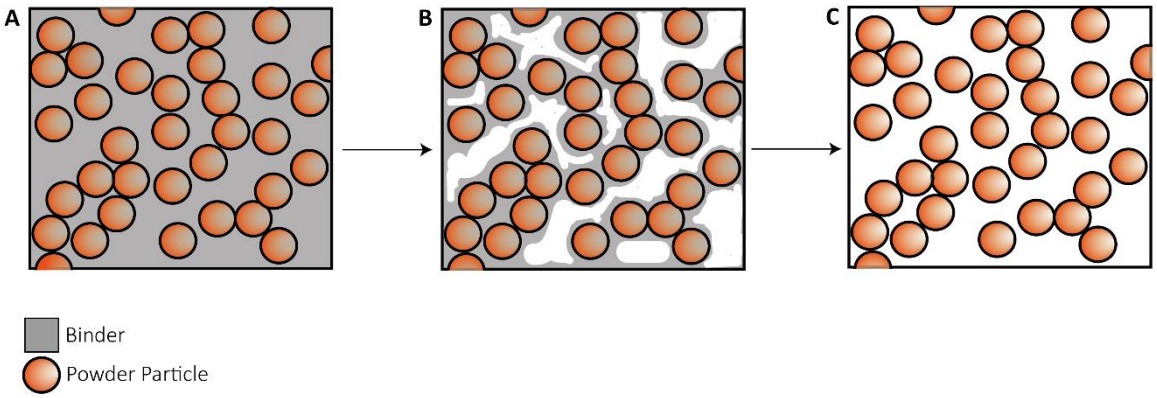

Figure 5 - Binder removal through a thermal cycle. A, feedstock at room temperature. **B,** polymers removal at lower temperature. **C,** binder complete removal at higher temperature

The solvent method utilises a solvent debinding unit to extract a solvent such as cyclohexane, followed by a thermal debinding step in the same furnace which will also be used for sintering [27], [34], [35]. Solvent removal consists of dissolution and diffusion;

hence it depends on time, temperature and particle characteristics like shape and size distribution. The solvents and the dissolved polymers diffusion are slower if the particles are smaller or more irregular, as these have a larger surface area of binder adhesion [35].

Finally, the catalytic process is much faster [33]. The main binder component is catalytically degraded from solid to vapor, as happens when acid vapours (like nitric acid) are added to polyoxymethylene-based feedstocks.

Both solvent and catalytic methods leave insoluble or non-degraded polymer remains before sintering, as a means of providing mechanical strength and shape preservation. Then, in a pre-sintering step, this skeleton is thermally removed, often at 200ºC to 600ºC according to its composition [33].

1.1.5. Sintering

Particles need to be no larger than 20 μm to undergo the deposition process. Fine particles yield the best results in FDMet, as they provide better flowing during injection and extrusion as well as better sintering, even though they can bond into larger chunks. A spherical particle shape mitigates internal-particulate friction while preventing particles from interlocking with one another, contributing to the creation of an isometric part structure. On the other hand, irregular particles provide denser sintering. An alternative is to use multimodal particle distributions, as these can increase the solid loading and thus the sintering density while decreasing sintering distortion. Hence, the powder characteristics affects many aspects, from sintering to the end product mechanical strength and surface finish [36].

Metal Injection Moulding (MIM) has certain requirements which some conventional powder technologies do not. In MIM, the binder transports the powder into the mould, forming the shape, which requires MIM powders, usually with d_{90} around 20 μm, to be much finer than conventional powders for metallurgy, sometimes with 150 μm. Nevertheless, conventional powders have about 25% fines where the fine powders are less than 45 μm. MIM has produced components with a d_{90} of about 45 μm, but these are among the largest and need special check rings in moulding machines with extra-large clearances. In micro MIM, commercially available powders can reach d_{90} of 2 μm, however these much finer particles have large surface area and thus surface energy, which impacts on the sintering and densification mechanisms [37].

Sintering is the final step in creating dense metal components, by thermally transforming metallic powders into bulk parts, where rearrangement, particle movement, and mass transport occur. The temperature is lower than the powder main constituent melting temperature, but usually within 70 to 90% of it, as occurs in PIM [33]. However, higher densities are obtained for temperatures closer to the melting point [38].

In sintering, highly porous parts made of large free surface particles with high surface energy undergo a heating process. Solid bonds known as necks [37] are then formed between the particles, reducing the surface energy and the part porosity as it gets higher density. However, the grains increase in size, hampering the speed and quality of the process.

In the end, final densities of almost 100% the theoretical value are only possible if a HIP thermal post-treatment is used [37], [39].

For nickel powder, greater relative densities can be achieved with smaller average particle sizes, for a given temperature (Figure 6) [40].It is expected that copper powders behave in a similar way, and so using HIP thermal post-treatment on a 50 μm particle size copper powder after it is processed at over 1080ºC could possibly yield an almost 100% relative density.

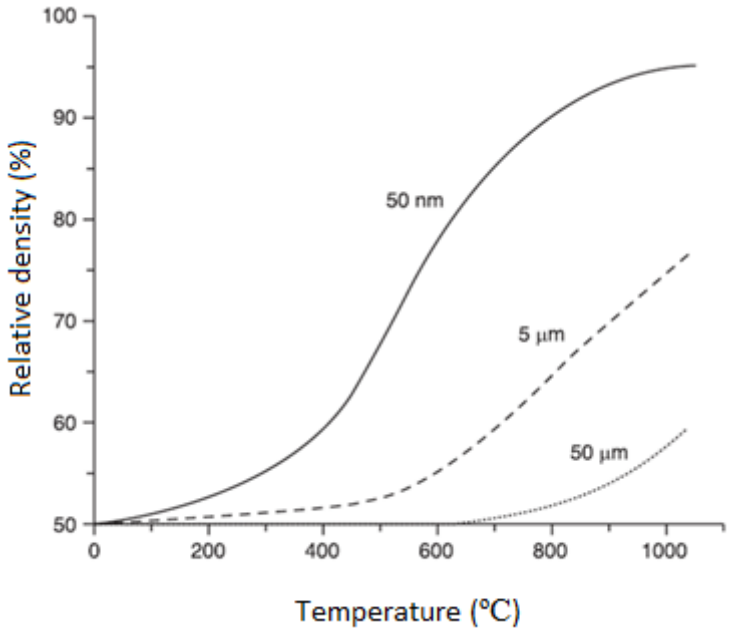

Figure 6 - Relative density and sintering temperature for three nickel powders with different average particle size (adapted from [40]**)**

Several mechanisms contribute to the mass transfer, including surface diffusion, lattice diffusion, grain boundary evaporation-condensation, viscous flow, and plastic flow

[37], all of which increase the formation of necks and strengthen the part. Some of these phenomena contribute to shrinkage and densification as well.

Surface diffusion creates surface smoothing, particle joining, pore rounding, yet no densification. The effects of diffusion occur due to sublimation and vapor transport, in case there is high vapor pressure in the material. Diffusion in the lattice and along the grain boundaries increases neck growth and density. If there is wetting, bulk viscous flow also increases density. Mechanical pressure creates plastic deformation [33].

After sintering is concluded, the decrease in porosity and increase in density always condition a certain degree of shrinkage of the part obtain through FDMet.

In PIM, the shrinkage is anisotropic [41], [42] due to the polymer orientation, which is conditioned by the injection moulding parameters [43].

In FDMet, gaps between deposited strands are also relevant. A higher number of these causes more shrinkage and less density of the end products [42]. The filler particles orientation also affects shrinkage [41]. The CAD should account for the unavoidable anisotropic shrinkage, as should the printing strategy. Failure to do so can cause excessive variation in the shrinkage and thus negatively impact on the end products.

If a liquid is present and wets the matrix, it creates a much faster path for mass diffusion. That is why excessive liquid during sintering can lead to collapse of the skeleton. On the other hand, the right amount of liquid can increase the speed of sintering and densification [37]. Covering copper powder particles with copper nanocrystals promotes fusion, initiating sintering faster [44].

1.1.6. Constructal Principle

Most of the moulding cycle is dedicated to mould cooling. This crucial phase impacts heavily on the production rate and on the end product quality [45], which makes the cycle time greatly dependent on the part cooling channel system. Its design can be improved using the constructal principle, by creating a first entry channel that splits into *n* evenly spaced secondary channels which then drain on the first channel (Figure 7), as it minimises flow resistance.

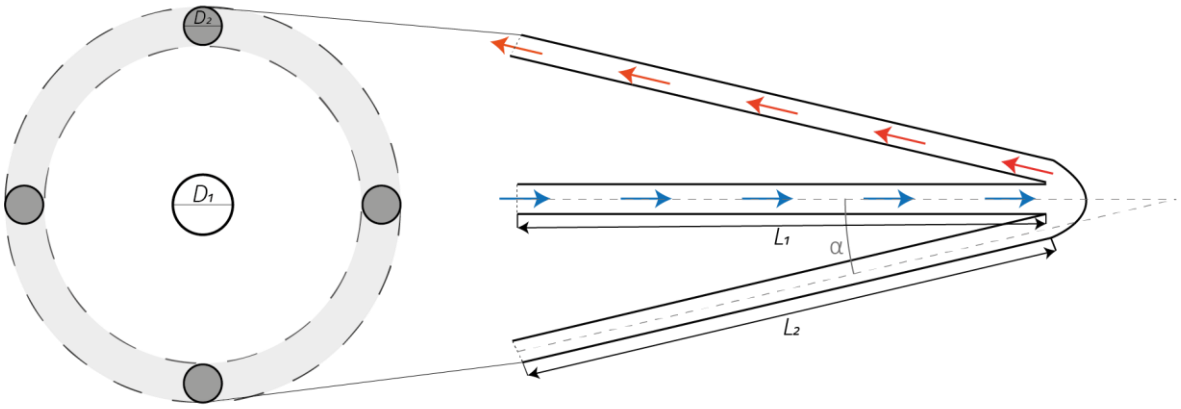

Figure 7 - Schematic example of the umbrella geometry with 4 return channels (adapted from [46]**)**

This principle states that "for a finite-size system to persist in time (to live), it must evolve in such a way that it provides easier access to the imposed currents that flow through it." [47], and it introduced the global geometric parameter known as Svelteness (1.1-1.3) [48]. It relates an external flow length scale with an internal one and is a function of the relative importance of local pressure losses in bends, junctions, contractions, expansions and friction pressure losses distributed along the channels, enabling the minimisation of local pressure loss over friction loss [46].

$$Sv = \left(\frac{L1/D1}{\psi(n,\alpha)}\right)^{\frac{2}{3}}, \tag{1.1}$$

with

$$\psi(n,\alpha) = \sqrt{\frac{\frac{\pi}{4}(1+n^{\frac{1}{3}}sec\,(\alpha))}{\left[tan(\alpha)\left[n\left(sin\left(\frac{\pi}{n}\right)+\frac{cot(\alpha)}{2}\right)\right]^{\frac{1}{2}}\right]^{3}}}, \tag{1.2}$$

and

$$\frac{D1}{D2} = n^{\frac{1}{3}}, \tag{1.3}$$

where *Sv* is the Sveltness, *D1* is the primary channel diameter, *D2* the secondary channel diameter, *L1* the primary channel length, α the secondary channels return flow angle and *n* the number of secondary channels.

Designing cooling channel systems for complex thin parts is difficult, but it can be made much easier and allow for more geometrical complexity using AM rather than subtractive methodologies. This is known as conformal cooling [49], [50] ,which makes the cooling more homogeneous and shortens its duration [51].

Currently, cooling system design is trending to vascularisation and constructal methodologies, as they produce channels better adapted to geometrically complex parts while reaching the necessary thermal balance.

Three geometric parameters must be considered when designing micro-mould cooling channels systems with this umbrella-like structure (1.4):

1. secondary channels diameter (D_2);
2. secondary channels return flow angle (α);
3. and the primary channel length (L_1).

$$n = floor\left[\frac{\pi L_1 \tan(\alpha)}{D_2}\right] \tag{1.4}$$

in which *n* is the number of secondary channels and *floor* is a function that rounds the result to the nearest integer less than or equal to that value.

2. MATERIALS, METHODS AND TECHNIQUES

2.1. Raw Material

2.1.1. Binder

The binder enables an easy moulding of the powders. Its thermal behaviour establishes the binding thermal cycle.

The binder system consists of a master binder, a backbone and additives[15]. In this study, their components/proportions were chosen in order to yield viscosity, stiffness and flexibility that allowed the filaments processing through FDMet.

The master binder used in this work was M1 from Atect® (Annex A), containing/consisting of polyolefin waxes and ethylenic polymers with numerical molecular weight. Its density was 965.5 kg/m3 and thermal process up to 600ºC is enabled to remove it completely. M1 was chosen as an interesting behaviour in the debinding and sintering stages has been reported [15], [52], [53], mostly because of its constituents different volatile properties and melting points.

The backbone was a thermoplastic elastomer (TPE), linear triblock copolymer based on styrene and ethylene/butylene (SEBS), grade G1651 from Kraton™; because of metallic powders being involved, TPE copolymer was added.

Accounting to the feedstock high viscosity and low flexibility, additives were necessary. As plasticiser, Diisodecyl Phthalate (IUPAC: bis(8-methylnonyl) benzene-1,2-dicarboxylate; C28H46O4) was used.

Although in research areas related to FDMet, such as Powder Injection Moulding (PIM), stearic acid (SA) has commonly been used as surfactant agent, it has recently been shown that an external plasticiser does not cause some undesired reactions between SA and the powder particles [15] while also increasing filament flexibility. TPE vol.% addition is limited by the accompanying increase in the feedstock viscosity.

2.1.2. Feedstock

Since powder contents is a function of mixing time, a Plastograph® Brabender® GmbH & Co. KG torque rheometer was used to optimise the feedstocks. The master binder required that the temperature was set at 180ºC. The total mixture time was 30 min, enough to usually achieve steady state, and the blades speed 30 rpm.

The final part geometrical and mechanical characteristics are greatly influenced by the feedstock metallic vol.% powder. Regarding PIM, it has been established that metallic powder content should be as high as possible while still attaining a steady regime and maintaining a torque value suitable for injection[15].

The PIM feedstocks form is the base line of this study. In similar powders, 60 vol.% was defined as the critical powder volume concentration (CPVC) [15], [52]–[54].

After CPVC definition, the feedstocks were prepared and then granulated in small pellets to expedite the feeding of the extruder.

2.2. Processing Methodologies

2.2.1. Feedstock Mixing

A Morton Z-Blade mixer was used to pulverise 2.35 kg of copper and mix it with a polymeric mixture (binder). A sample was taken and used for torque rheometry in a Brabender® Plastograph® W 50 mixer (Figure 8), in order to evaluate the CPVC (cf. Appendix A).

Figure 8 - Brabender® Plastograph® W 50 mixer

This equipment has a dynamometer attached to the mixer rotating blades and records torque and stock temperature versus time for each material.

The dynamometer was calibrated by rotating the blades inside the empty chamber. Next, the binder was introduced into the chamber, decreasing the temperature, and then the different powders sequentially. Once homogenisation occurred, at fixed speed and sufficient temperature, the torque decreased to reach a steady state which became unstable upon adding the next powder, before it homogenised once again. This process was repeated until reaching the CPVC, that is the maximum fraction of solids which could still be homogenised and reach a steady state [52], [53].

The experiment was done for 30 minutes at 30 rpm and 180ºC, according to the binders thermal analysis [52]. This was beneath the binder degradation temperature of 200ºC.

2.2.2. 3D Printing

The insert CAD was assembled using Autodesk® Inventor® Professional 2019. Afterwards, the G-Code was obtained through PrusaSlicer 2.0 and then printed by Repetier (developed by Hot-World GmbH & Co. KG).

The green inserts were produced using a Prusa i3 MK3 (Figure 9) with the following custom parameters:

- maximum build volume: 250 x 210 x 210 (mm);
- filament diameter: 1.75 mm;
- nozzle size: 0.4 mm;
- maximum extruder/heated bed temperature: 300/100 (ºC);
- minimum layer height: 0.05 mm.

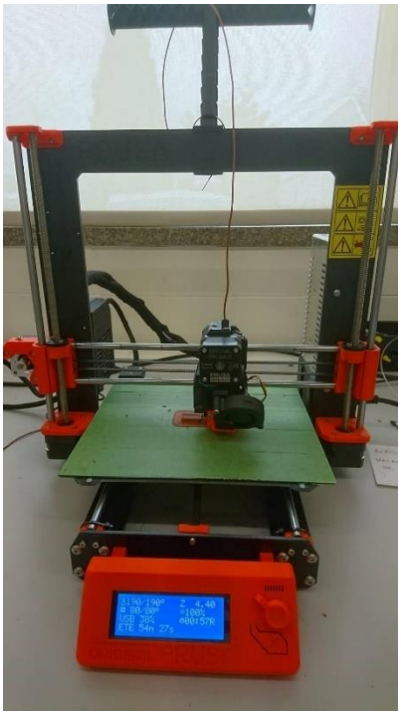

Figure 9 - Prusa i3 MK3 FDMet Equipment for FDMet

2.3. Characterisation Techniques

2.3.1. Gas Pycnometry

Gas Pycnometry is a non-destructive technique that uses the gas displacement method to measure volume and calculate the material true density. Density is the weight to volume ratio (excluding voids).

In this study, an Accupyc 1330 helium pycnometer from Micromeritics was utilised, with helium as the displacement medium due to its properties similar to ideal gases. It uses pressure changes of the displacement medium in a known volume to obtain the density.

2.3.2. Laser Diffraction Spectroscopy (LDS)

Laser diffraction spectrometry (LDS) was used to evaluate the powder particle size distribution (PSD) in a Malvern Instruments Mastersizer 3000, as required by the ISO 13320-2009 standard. According to the Fraunhofer diffraction theory, the angle of diffraction of light scattered by a particle is inversely proportional to the particle size, thus allowing the calculation of the PSD. Water was used as dispersion medium.

The results were represented as the particle diameter which is greater than 10, 50 and 90 % of the distribution (in µm), respectively d_{10}, d_{50} and d_{90}. The distribution width, S_w, is related to the cumulative distribution slope and is similar to the standard deviation of the distribution [55]. A smaller value of S_w (2.1) corresponds to a wider PSD. High S_w values, namely around 4 or 5, correspond to an increase of processing difficulties, in opposition to powders with S_w values of around 2 [52], [55]–[57].

$$S_w = \frac{2.56}{\log_{10}(d_{90}) - \log_{10}(d_{10})} \tag{2.1}$$

2.3.3. X-rays Diffraction (XRD)

To identify the material phases, XRD was used.

This non-destructive technique working principle is based on the constructive interference of monochromatic X-rays generated by a cathode ray tube on a crystalline sample.

The interaction produces a diffracted ray when conditions satisfy Bragg Law (2.2), which relates the wavelength of electromagnetic radiation to the diffraction angle and the lattice spacing in the crystalline sample [52].

$$n_b\lambda = 2d_p \sin\theta \tag{2.2}$$

where,

n_b – diffraction order (positive integer)

λ – wavelength of the incident wave

d_p – interplanar distance between lattice planes

θ – angle of diffraction (scattering angle)

In this study, the equipment used was XPert Pro from PANalytical coupled with a PW 3020/00 goniometer, with current and voltage of 35 mA and 40 kV respectively.

2.3.4. Optical Microscopy (OM)

The microstructure of the green and final inserts has been observed through a versatile upright microscope for material analysis with Leica DM4000 M LED connected with a LEICA MC190 HD camera (Figure 10).

This equipment grants a maximum amplification of 1000x and provides full-colour images and Full-HD movie clips from the samples.

Figure 10 - Leica DM4000 M LED connected with a LEICA MC190 HD camera

2.3.5. Scanning Electron Microscopy (SEM)

The scanning electron microscope scans an object through the detection of secondary electrons which result of inelastic interactions between the samples atoms and a focused electron beam.

A Quanta 400 FEG ESEM equipped with EDS, EDAX Genesis X4M system with beam energy of 15 keV was used to evaluate the surface topography and composition of the inserts.

2.3.6. Infinite Focus Microscopy (IFM)

IFM is a non-contact optical 3D surface measurement system which carries out dimensional metrology and surface roughness measurements with high repeatability and vertical resolution of up to 10 nm. This technique uses the focus-variation principle, which combines an optical system small depth of focus with a vertical scanning.

In the present study, shrinkage, geometrical precision and surface roughness of the green and final inserts were evaluated by the Infinite Focus Microscope from Alicona Imaging GmbH.

3. RESULTS AND DISCUSSION

3.1. Powder Characterisation

For any additive manufacturing study, it is imperative to characterise the powder before processing, regarding size and particle size distribution, shape and structure (4Ss) [13].

3.1.1. Size and Particle Size Distribution

The particle size Gaussian distribution, median value and distribution width of copper powders acquired through LDS are presented in Figure 11 and Table 2.

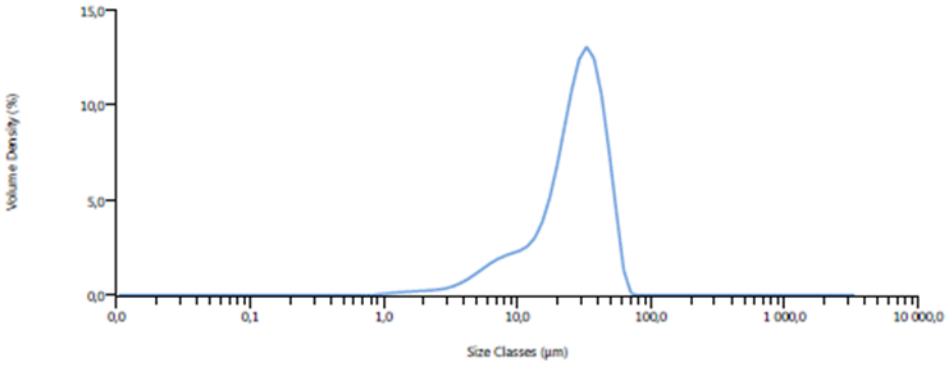

Figure 11 - Particle size distribution of copper powder (Ecka) particles

Table 2 - Characteristics of copper powder (Ecka) particles

d_{10} [µm]	d_{50} [µm]	d_{90} [µm]	ρ [kg/m^3]	S_w
8.57	28.00	46.60	8896	3.48

Copper powder (Ecka) has a bimodal distribution concerning its granulometry. Moreover, particle size distribution width (S_w) is higher than the suitable value (cf. Chap. 2). In fact, powders with a S_w value around 2 are the easiest to mould. Although a S_w of 5 has been considered the maximum suitable for moulding [52], there are reports of good moulding performance using metals (i.e. SS 316L) with S_w values similar to the copper powder calculated value [58].

Nevertheless, a median particle size (d_{50}) of 28 µm can be unsuitable for sintering, due to low particle surface area, which is the main thermodynamic driving force for sintering.

3.1.2. Shape

The shape factor takes into consideration the morphology of the powder particles and has direct implications in interparticle friction [36], wettability and dimensional variation during the manufacturing process.

Figure 12 shows that the powder mostly consists of spherical particles, meaning a shape factor close to 1. Nevertheless, spherical particles should reduce the sintered density needed to maximise thermal conductivity which is the target of this study.

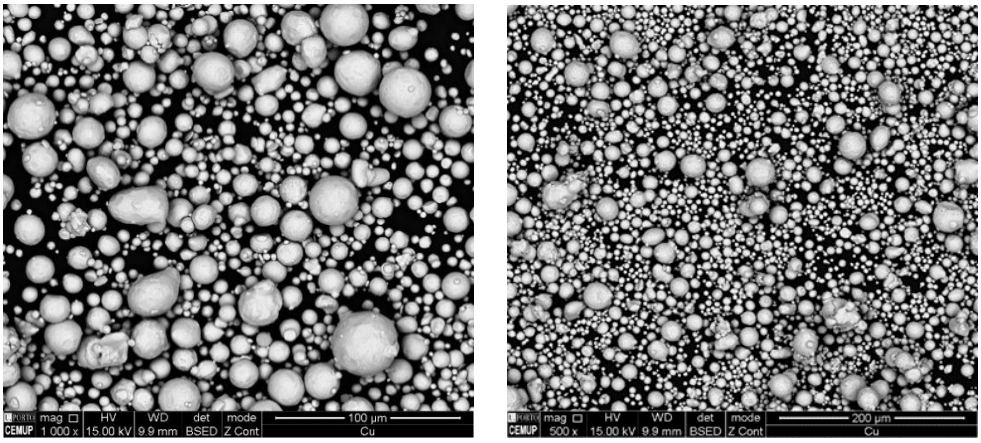

Figure 12 - Micrographies (SEM) of copper powder particles (Ecka)

3.1.3. Structure

Figure 13 shows the diffractogram of copper powders.

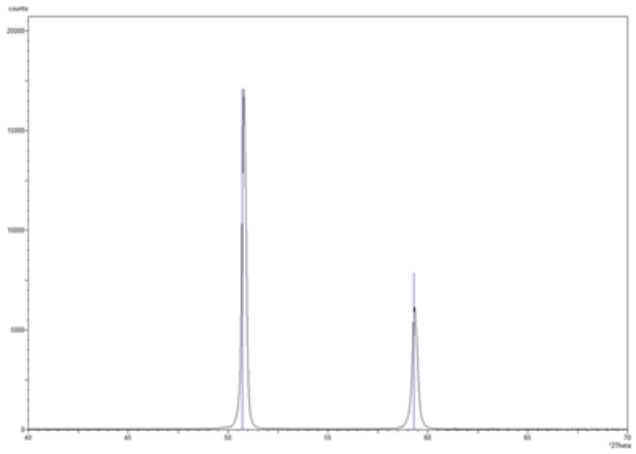

Figure 13 – X-ray diffractogram of copper powder

The relative intensity of the peaks in the diffractogram is similar to the peaks of bulk pure copper, without any anisotropy. In addition, no peaks related to the presence of oxides, carbides or other impurities/contaminants were identified. The purity of copper powder surface is essential to achieve the best density after sintering [59].

3.2. Filament Manufacturing

3.2.1. From Powder to Feedstock

The feedstock was mixed using copper powder, binder and other additives (Table 3) [15], [52].

The mixture was processed in a Z-Blade in two stages, where the oil temperature was 180ºC. In the first stage, metallic powder and master binder (M1) were blended during 10 minutes. Then, thermoplastic elastomer (TPE) and dispersant (plasticiser) were added without stopping the machine and the mixing continued for 20 minutes, resulting in a feedstock with different percentages in volume (vol. %) (Table 3).

Table 3 – Percentages of each additive in feedstock

Component	Vol. %	Mass (g)
Copper	60	2351
M1	31	131
TPE	7	31
Dispersant	2	8
Final Feedstock	100	2522

Afterwards, the final mixture was granulated using a Hellweg Maschinenbau Disc Mill, yielding a feedstock true density of 5480 kg/m^3 (measured through gas pycnometry).

3.2.2. From Feedstock to Filament

The feedstock was extruded into filament through a Brabender® GmbH & Co. single screw extruder, with five controlled heated zones and a nozzle diameter of 1.75 mm.

The screw rotation speed was of 5 rpm and the temperature increased 5°C between the heated zones, reaching 185°C in the last zone.

In order to ensure the highest homogeneity along the filament, the height of the filament drop was fixed at 0.15 m. Long lengths make the filament more likely to break, while short ones cause the filament to not curl into a wire form.

The width of the wire is another important factor. Although slight variations do not have significant consequences, a wider filament is less likely to break during printing, albeit being an uncompact solution. A compromise is thus necessary.

The filament produced had an acceptable diameter of 1.70 ± 0.03 mm, considering that several industry standard filaments have diameters from 1.70 mm to 1.80 mm with ± 0.05 mm resolution [25]. Comparing to certain commercial filaments, a diameter consistency with ± 0.03 mm resolution can lead to minor problems regarding the printed parts/systems quality.

The extruded filament could easily be curled and fit into a coil if moderately heated throughout. This is an indicator of the plasticity needed for the filament to be correctly extruded and to reduce the need for hand feeding the filament, in order to guarantee continuous flow. However, at room temperature the filament is extremely fragile, requiring careful handling. In this work, a previous heating of the printing bed up to 40°C allowed to attain the best building properties, scaling down the number of hand feeding operations and clogging.

3.3. FDMet

3.3.1. Computer-aided Design (CAD) Specifications

Besides the 3D printing equipment, FDMet also requires a digital design (CAD) to fabricate the selected parts. Moulding inserts were the moulding components used as concept proof of FDMet quality. These inserts are usually cooled in order to promote the injection rate and the quality of the injected plastic (i.e. brightness). The technologic development obliges to use cooled inserts. Different approaches have been adopted, like conformal cooling. However, the tendency is to improve the cooling efficiency by other cooling systems, where the geometry becomes more and more complex. There is only one process capable of producing inserts with these specifications – AM.

Figure 14 illustrates the insert CAD obtained using Autodesk® Inventor® Professional. Figure 15 is a cross section of the insert and Figure 16 is a representation of the cooling channels in detail.

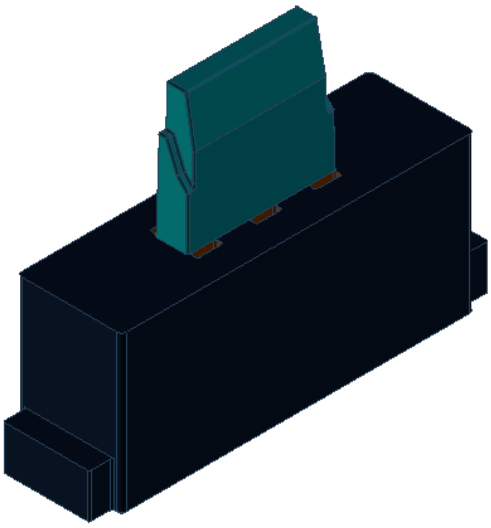

Figure 14 - CAD isometric view of an insert

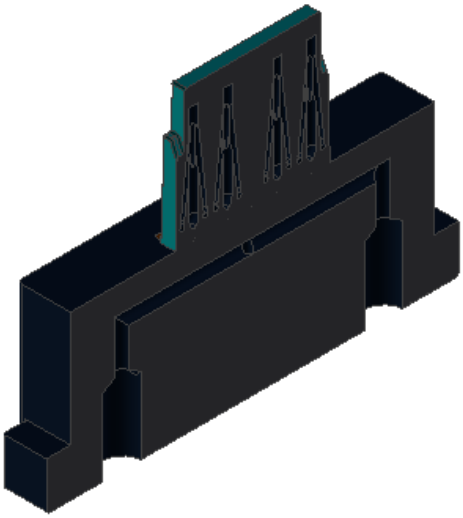

Figure 15 - CAD cross section of an insert

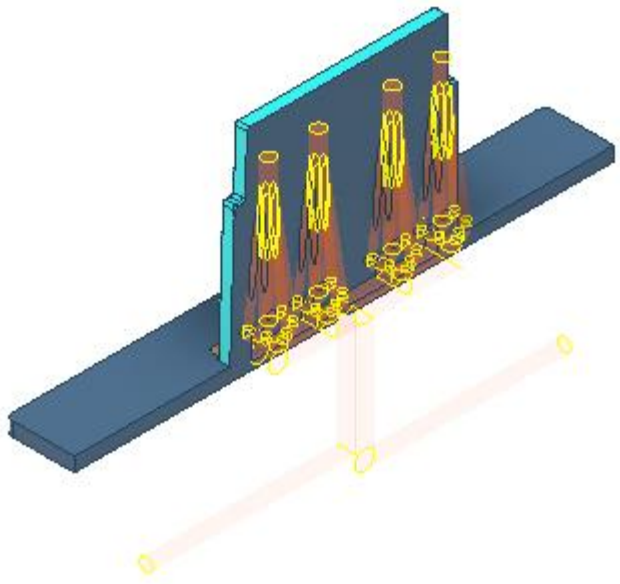

Figure 16 – Schema of cooling channels

In order to apply the constructal principle to the cooling system of the insert, the channels were designed with the parameters summarised in Table 4.

Table 4 – Cooling channels design parameters

Parameter	Value
Number of secondary channels (*n*)	7
Primary channel length (L_1) [mm]	10.000
Primary channel diameter (D_1) [mm]	0.956
Secondary channel diameter (D_2) [mm]	0.500
Secondary channel return flow angle (α)	6.47 º

After the CAD assembly of the designs of the insert and the cooling channels, the format was exported to Standard Tessellation Language (STL), developed by 3D Systems®, in order to define the printing code (G-Code). In this conversion process, the quality of the details may be reduced depending on the software and parameters selected.

The CAD has to consider the 3D printing equipment limitations, specifically the layer height and diameter of the extruded filament. A lack of material in the profile of the insert (Figure 17) could be the result of mismatching between the CAD and the process

limitations, due to the wall thickness being thinner than the extruded filament diameter. Then, the program will not consider that part eligible to print.

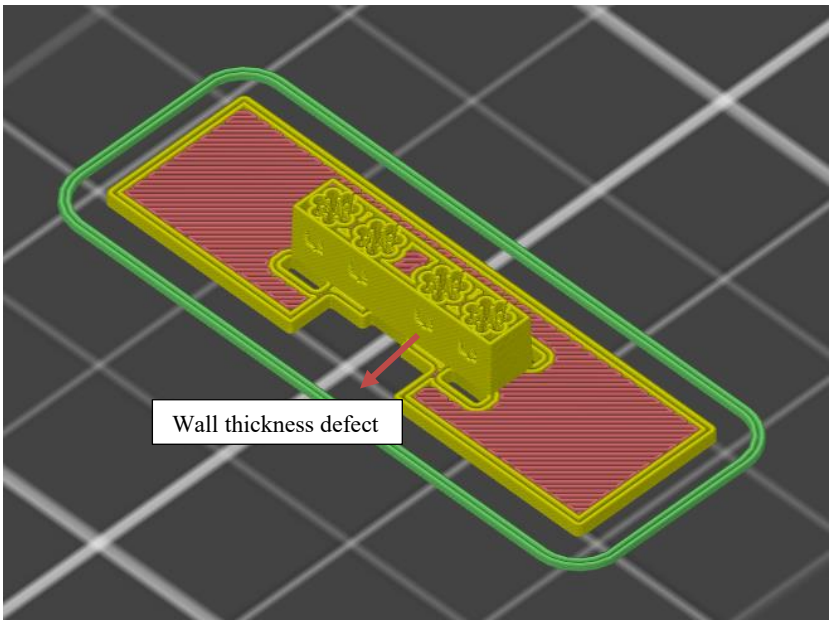

Figure 17 - G-Code representation of a copper insert with umbrella-shaped channels showing wall thickness defects

3.3.2. Parametrisation and Printing Tests

In order to establish the limits of the 3D printer selected and optimise printing parameters, copper components with different geometries have been processed before the manufacturing of the final inserts. Cubes with different infill percentages and patterns, prisms with several proportional holes aligned, helical gears and other parts of high geometrical complexity with rough curves and sharp angles were tested (cf. Appendix B). The purpose of these prototypes was to define the following parameters:

- brim and skirt adjustments to maximise adhesion with the lowest waste of material;
- the smallest hole diameter possible before occurring obstruction of the cooling channels;
- and, heated bed and extruder temperatures during deposition.

The fabrication of copper cubes with different parameters (Figure 18) lead to the conclusion that only 3 brims were required to grant a uniform flow rate without the need for

skirts in components with at least 20 mm of width. Furthermore, the bed temperature should not be higher than 80ºC as the copper cubes started to detach from the base surface. The nozzle temperature of 190ºC was the most suitable, according to the bibliography [60].

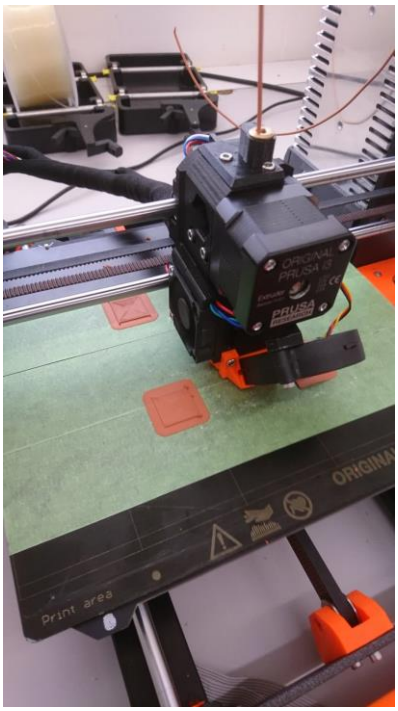

Figure 18 - Production of five copper cubes made with different parameters

Figure 19 shows prisms with several holes aligned with a hole diameter increment of 0.04 mm, starting at 0.02 mm and finishing at 0.30 mm. The hole with diameter 0.02 mm was completely obstructed. A diameter of 0.06 mm already allowed the partial flow of the cooling fluid, but diameters of 0.10 mm or more were completely unclogged. Therefore, it is possible to build inserts with secondary channels with at least 0.10 mm of diameter following the constructal principle.

Comparing to Selective Laser Melting, where laser beam diameter is usually around 0.08-0.09 mm, FDMet of copper shows great promise regarding the production of complex cooling channels with great detail, as low as 0.10 mm, using a 0.4 mm nozzle. Due to melting properties, SLM or other melt-based processes can hardly achieve an open channel for conductive materials.

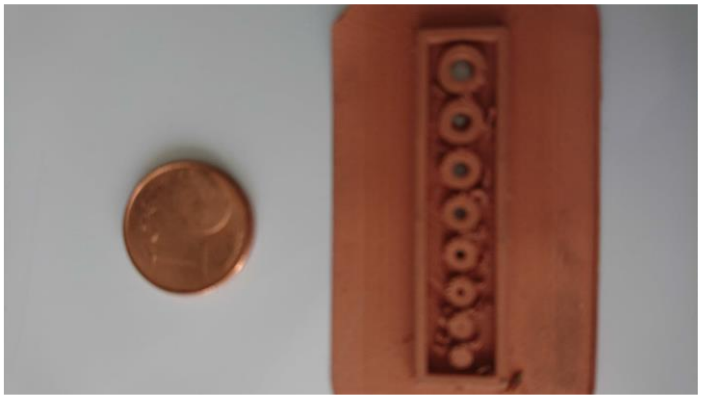

Figure 19 - Prism with several holes aligned, from 0.02 mm to 0.300 mm with an increment of 0.04 mm

3.3.3. From Filament to Green Part

From the previous tests to the desired green copper inserts (Figure 20), the different layers in vertical plane become visible. These could contribute to warpage, but that is not evident.

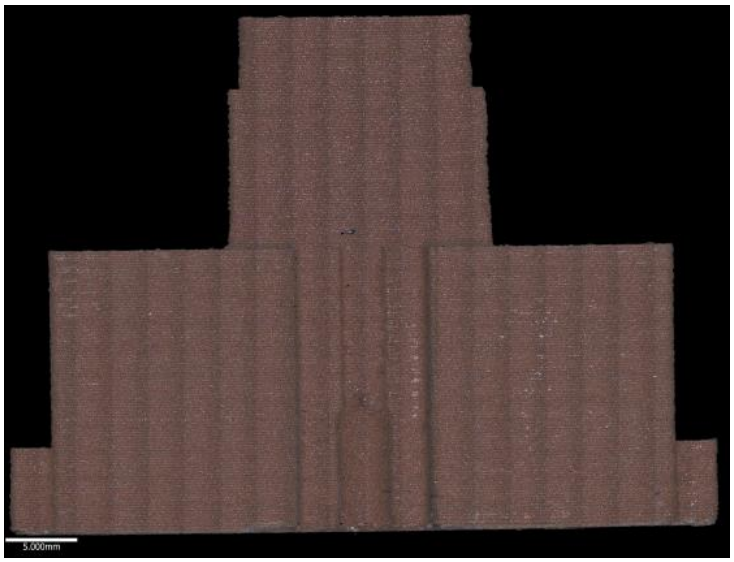

Figure 20 - Green copper insert

Horizontal and vertical insert tips were made with conformal and constructal channels with the purpose of observing them through OM. Figures 20 to 25 show different zones of the insert tips.

Channels for the cooling fluid (water) were produced, and they did allow it to flow freely. Unlike the vertical insert tips channels, the holes circularity in the horizontal tips (Figure 22) are a function of the selected height and x and y machine resolution. Since

the value of height is never close to x and y axis resolution, it can never produce a perfect horizontal channel. This problem is transversal to all additive manufacturing processes. However, by reducing the nozzle diameter and layer height it is possible to make the holes contour closer to a circumference.

Some of the holes in the insert tips got obstructed (Figure 25). This occurred in the first layer due to the lack of adhesion to the printing bed surface. Furthermore, the first layer requires a greater amount of material in order to promote the adhesion with the following layers. A third reason for the hole occlusion can be attributed to the fact that the extruded filament in FDMet behaves like a paste, and so it can enlarge to the sides after being deposited. In the second layer, the behaviour of the extruded filament is different. The internal holes have not this problem during the manufacturing of the full inserts.

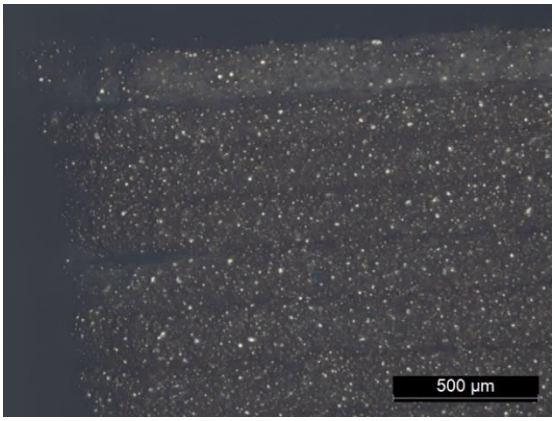

Figure 21 - Insert tips upper-left corner lateral topography

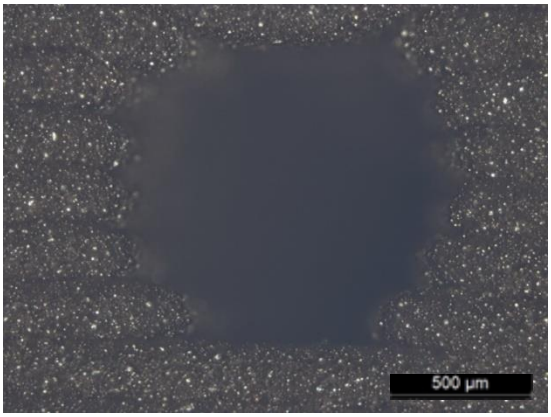

Figure 22 - Horizontal insert tips channel opening detail topography

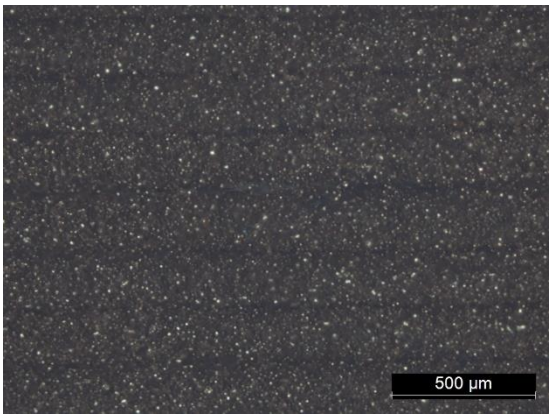

Figure 23 - Insert tips lateral surface topography

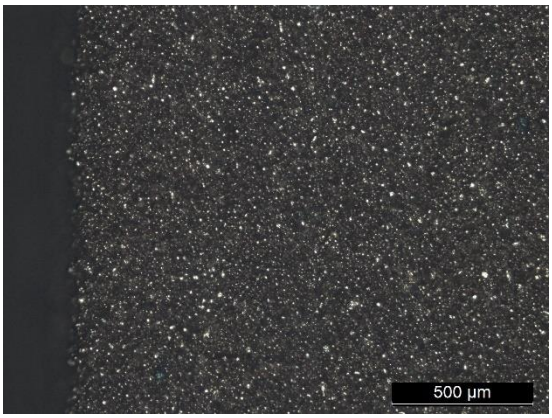

Figure 24 - Insert tips top surface topography

Figure 25 - Vertical insert tips obstructed channel opening detail topography

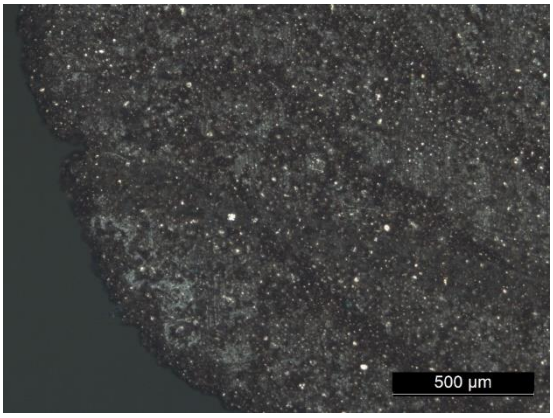

Figure 26 - Insert tips upper-left corner top topography

3.4. Debinding and Sintering

The debinding and sintering thermal cycles (Figure 27) were defined considering the feedstock Thermogravimetric Analysis (TGA) and copper powder thermal behaviour [15], [52], [53].

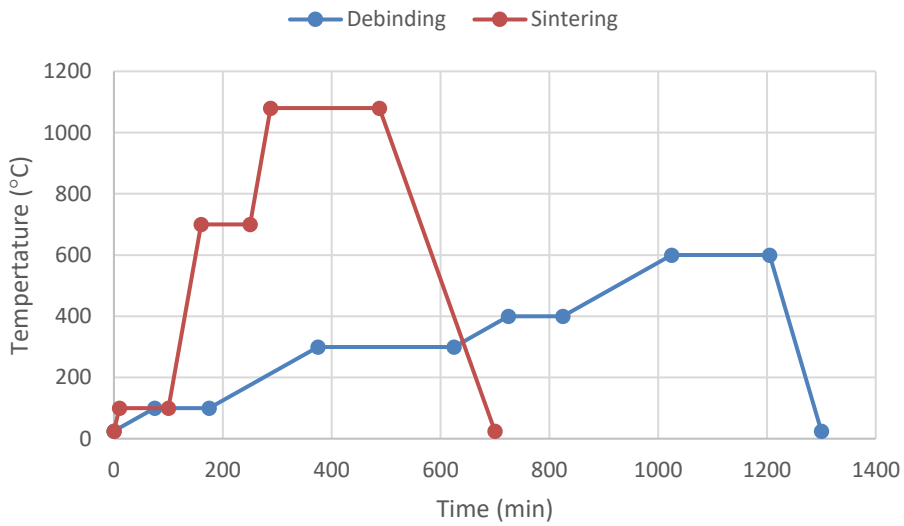

Figure 27 - Debinding and sintering thermal cycles with heating rates of 1°C/min and 10°C/min

An atmosphere of argon, with or without hydrogen, could be the solution. The hydrogen is beneficial because it can reduce the existing oxides in the copper powder surface, forming water that disappears during sintering. However, argon is an inert element

and it will not disappear during sintering, making the maximum density impossible to attain. Moreover, if the particle size dimensions are not suitable, as in this study, full sintering becomes difficult and the presence of argon could contribute to decreasing the sintering effect. The argon is retained in the pores of the brown part, and they have no possibility to diffuse argon into copper, during sintering. Thus, the porosity is difficult to disappear. The best option is to use only hydrogen, but this gas could contribute to explosions.

In this study, a vacuum furnace was used since it was expected to produce a final insert with high density [61], [62]. However, during the sintering step, layer separation occurred in the insert because of the lack of pressure related to the step-by-step process.

3.5. FDMet Insert Characterisation

3.5.1. Geometry and Dimensions

Before the debinding and sintering stages, the main dimensions of the insert profile were evaluated through IFM (Figure 28 and Table 5).

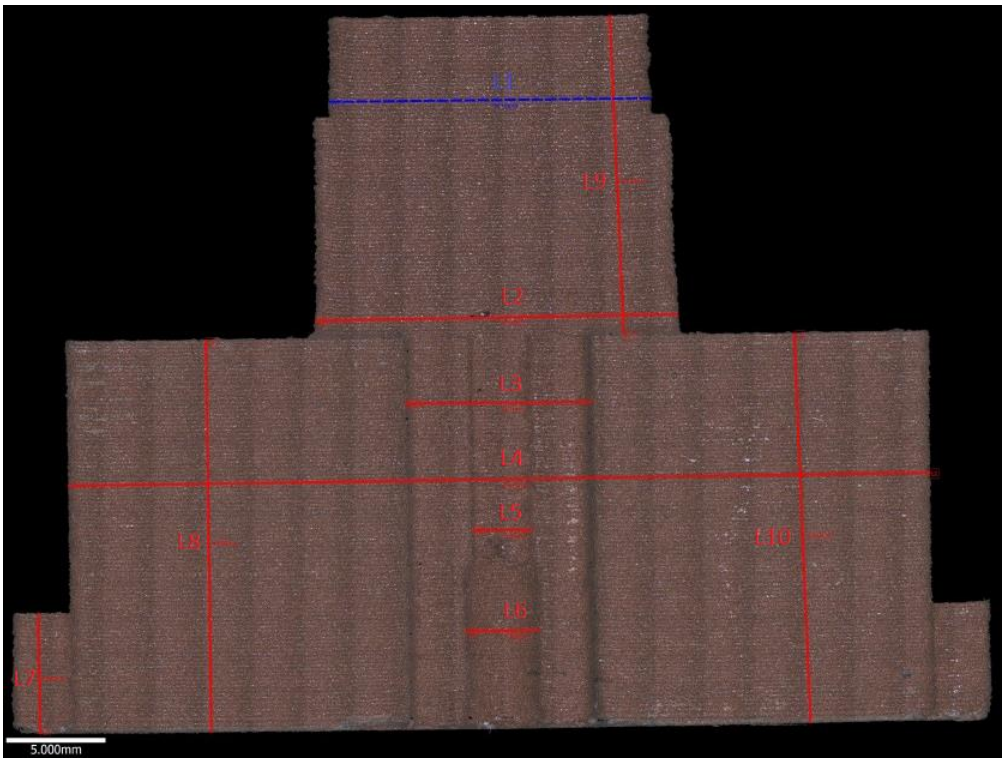

Figure 28 - IFM caption of the green insert

Table 5 - Comparison of dimensions between the CAD and the green insert

Dimension [mm]	CAD	Green Insert	Percentual Difference (%)
L1	14.300	16.119	11.28
L2	16.100	18.198	11.53
L3	8.000	9.310	14.07
L4	38.000	43.370	12.38
L5	2.800	2.914	3.91
L6	3.450	3.638	5.17
L7	5.000	5.982	16.42
L8	17.000	19.683	13.63
L9	14.838	16.043	7.51
L10	17.000	19.542	13.01

From these results, it can be concluded that the green insert dimensions exceed the CAD planned dimensions on an average of 10.81 %. However, after the sintering stage, the part is expected to have a volumetric shrinkage from 12% to 18% [36], meaning that the final insert volume should be between 11.5 % to 19.7 % larger than the CAD. For this reason, it is necessary to consider each of these values when drawing the CAD and not just the average percentual difference, in order to ensure the green component has the desired dimensions.

Comparing the green insert with the CAD, it is also noticeable that the inconsistent dimensional variation proves anisotropic behaviour. The main reason can be attributed to the significant size variation due to the insert geometry. However, a heterogenic filament or the different printing orientations during deposition may also cause this anisotropy.

Furthermore, the dimensions L8 and L10 both correspond to the insert height excluding the tip. The difference between these two values is 181 µm, which means a high precision of flatness for such a soft material as copper [63], [64].

3.5.2. Surface Roughness

The green insert profile surface topographical analysis was preformed through IFM (Figure 29 toFigure 31). The roughness values (Ra, Rq and Rz), summarised in Table 6, show to be lower than other values obtained for copper by FDMet (Rz ≥480 µm against Rz=174 µm).The demonstration of the possible character of FDMet near net shape is evident when comparing to other copper additive processing (SLM or other techniques) [8], [36], [65]–[67].

Figure 29 - Green insert lateral surface (IFM)

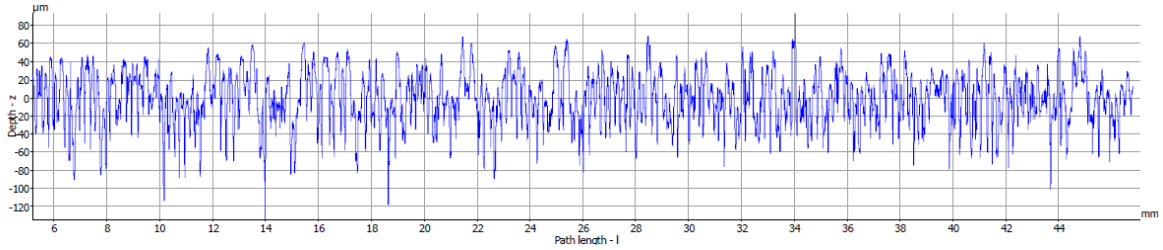

Figure 30 - Roughness profile of the green insert lateral surface (IFM)

Table 6 - Roughness profile of the green insert lateral surface obtained through IFM

Profile Roughness Parameter	Value [µm]
Ra	23.5
Rq	29.3
Rz	174.5

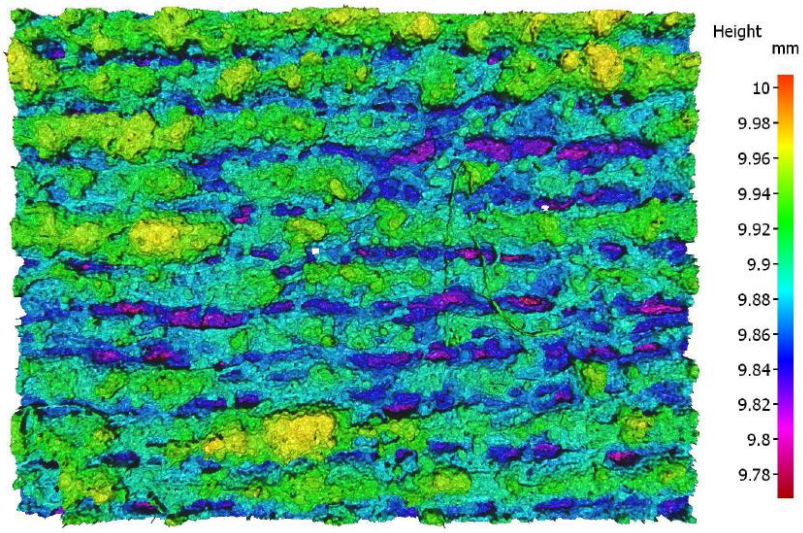

Figure 31 - Green insert lateral surface (IFM), with colour scale

CONCLUSIONS

This study shows that copper parts/systems can be produced through FDMet from feedstocks containing 60 vol. % of copper powder and 40 vol. % of different selected polymers (binder and other additives that can assure plasticity and stiffness). However, an unsuccessful sintering stage precluded has shown that an extended study must be made in this area to achieve fully dense parts.

The copper filament produced was suitable for FDMet, but its high thermal conductivity predisposes to blockage of the extrusion channel due to filament properties and extrusion method. Special care must be taken when introducing the parameters and the extrusion head should not be exposed to temperatures above 150ºC when idle. Otherwise, the filament in the extrusion channel can achieve the glass transition temperature of the binder, compromising the continual pull of the filament and causing the upstream portions to break, urging the need for continuous extrusion or high filament cooling.

In this work, hole diameter could be as low as 0.1 mm without causing obstruction of the cooling channels with an 0.4 mm nozzle, except the first layer, where layer adhesion may largely obstruct cooling channels, urging the need for post-processing the green part.

The major problems in the sintering step were independent of the extrusion-based process, as they were caused by the geometry of the inserts. The inconsistency among the green insert dimensions led to different contraction patterns, causing the thinner portions to fragmentise and the smaller portions to detach from larger ones. Furthermore, vacuum cannot be used in this step-by-step process because the lack of pressure causes layer separation. For this reason, it is necessary, if possible, to use hydrogen as the atmosphere of the sintering furnace and to apply hot isostatic pressure (HIP) afterwards to obtain a final component with around 100% density.

FUTURE WORK

First of all, it is necessary to optimise the sintering atmosphere. Afterwards, it is utterly important to study the mechanical behaviour of the produced inserts.

The results achieved using a nozzle with 0.4 mm of diameter were satisfactory, but to optimise the thermal distribution of the cooling channels, a study concerning a nozzle with 0.25 mm or lower is required.

Since the main objective is to favour the heat exchange in the connecting part of the insert, it may be interesting to produce bimaterial inserts using copper as heat transfer and steel as support through FDMet, upgrading the mechanical resistance of the insert while keeping a high thermal conductivity.

Moreover, the addition of graphene to the feedstocks in order to maximise the heat transfer in the inserts is also a case of study. FDMet could be the solution to use carbon allotropes without their destruction due to excessive temperature.

BIBLIOGRAPHY

[1] ISO/ASTM 52900:2015(en), Additive manufacturing — General principles — Terminology. 2015.

[2] E. Forrest and Y. Cao, "Digital Additive Manufacturing: A Paradigm Shift in the Production Process and Its Socio-economic Impacts," *Eng. Manag. Res.*, vol. 2, no. 2, pp. 66–70, 2013.

[3] N. Hopkinson, R. J. M. Hague, and P. M. Dickens, *Rapid Prototyping - An Industrial Revolution for the Digital Age*. John Wiley & Sons, Ltd, 2006.

[4] Deloitte, "Challenges of Additive Manufacturing Why companies don't use Additive Manufacturing in serial production," 2019. .

[5] M. Yakout, M. A. Elbestawi, and S. C. Veldhuis, "A Review of Metal Additive Manufacturing Technologies," *Solid State Phenom.*, vol. 278, pp. 1–14, 2018.

[6] J.-P. Kruth, P. Mercelis, J. Van Vaerenbergh, L. Froyen, and M. Rombouts, "Binding mechanisms in selective laser sintering and selective laser melting," *Rapid Prototyp. J.*, vol. 11, no. 1, pp. 26–36, 2005.

[7] L. P.A., S. E.V., and A. A.M., "Selective Laser Melting of Copper," *Mater. Sci. Forum*, vol. 843, pp. 284–288, 2016.

[8] A. A. Saprykin, N. A. Saprykina, and A. A. Saprykin, "Analysis and prediction of copper surface roughness obtained by selective laser melting Analysis and prediction of copper surface roughness obtained by selective laser melting," *IOP Conf. Ser. Mater. Sci. Eng.*, vol. 441, no. 4, 2018.

[9] J. Mireles, D. Espalin, D. Roberson, B. Zinniel, F. Medina, and R. Wicker, "Fused Deposition Modeling of Metals," *23rd Annu. Int. Solid Free. Fabr. Symp. - An Addit. Manuf. Conf.*, pp. 836–845, 2012.

[10] C. 2020, "Indústria 4.0 a quarta revolução industrial." [Online]. Available: http://www.poci-compete2020.pt/destaques/detalhe/Industria_4ponto0. [Accessed: 15-May-2019].

[11] U. M. Dilberoglu, B. Gharehpapagh, U. Yaman, and M. Dolen, "The role of additive manufacturing in the era of Industry 4.0," *Procedia Manuf.*, vol. 11, no. June, pp. 545–554, 2017.

[12] D. A. C. Gatões, "Processos híbridos step-by-step para produção de componentes metálicos com geometrias complexas," Universidade de Coimbra, 2016.

[13] P. Grootenhuis, R. W. Powell, and R. P. Tye, "Thermal and Electrical Conductivity of Porous Metals made by Powder Metallurgy Methods," *Proc. Phys. Soc.*, vol. 65, no. 7, pp. 502–511, 1952.

[14] S. H. Masood, "Advances in Fused Deposition Modeling," *Compr. Mater. Process.*, vol. 10, pp. 69–91, 2014.

[15] F. J. S. Cerejo, “Development of filaments for 3D printing of steel parts,” University of Coimbra, 2018.

[16] I. Gibson, D. W. Rose, and B. Stucker, *Additive Manufacturing Technologies Rapid Prototyping to Direct Digital Manufacturing*. Springer, Boston, MA, 2015.

[17] A. R. T. dos S. Farinha, “Consolidação mecânica com explosivo como pulverotecnologia para microfabricação,” Universidade de Coimbra, 2013.

[18] J. Kähler, N. Heuck, A. Wagner, A. Stranz, E. Peiner, and A. Waag, “Sintering of Copper Particles for Die Attach,” *IEEE Trans. COMPONENTS, Packag. Manuf. Technol.*, vol. 2, no. 10, pp. 1587–1591, 2012.

[19] J. Niittynen and M. Mäntysalo, “Characterization of Laser Sintering of Copper Nanoparticle Ink by FEM and Experimental Testing,” *IEEE Trans. COMPONENTS, Packag. Manuf. Technol.*, vol. 4, no. 12, pp. 2018–2025, 2018.

[20] C. D. A. Inc., “Cu,” 2019. [Online]. Available: https://www.copper.org/. [Accessed: 15-Jun-2019].

[21] A. Heidarzadeh, M. Jabbari, and M. Esmaily, “Prediction of grain size and mechanical properties in friction stir welded pure copper joints using a thermal model,” *Int. J. Adv. Manuf. Technol.*, vol. 77, 2015.

[22] A. Muizz, M. Noor, N. Hisyamudin, M. Nor, and S. Yokoyama, “Solubility of Nitrogen Gas into Molten Copper at Temperature Range of 1,993 K to 2,443 K,” *High Temp. Mater. Process.*, vol. 36, no. 10, pp. 1035–1038, 2017.

[23] R. German, “Carbon Control: An important discriminant in Metal Injection Moulding,” *Powder Inject. Mould. Int.*, vol. 9, no. 1, pp. 31–41, 2015.

[24] O. Barabash and Y. Koval, “Crystal Structure of Metals and Alloys,” *Kiev Nauk. Dumka*, 1986.

[25] M. Petch, B. Jackson, T. Vialva, U. Iftikhar, and A. Essop, “3D Printing Industry,” 2017. [Online]. Available: https://3dprintingindustry.com/news/first-look-and-test-prints-of-new-prusament-3d-printing-filaments-140286/.

[26] J. Flynt, “3D Insider,” 2018. [Online]. Available: https://3dinsider.com/3d-printer-parts.

[27] J. Gonzalez-Gutierrez, S. Cano, S. Schuschnigg, C. Kukla, J. Sapkota, and C. Holzer, “Additive Manufacturing of Metallic and Ceramic Components by the Material Extrusion of Highly-Filled Polymers: A Review and Future Perspectives,” *Materials (Basel).*, vol. 11, no. 5, 2018.

[28] D. Chakravorty, “STL File Format for 3D Printing—Simply Explained: Are There Any Alternatives to the STL File Format?” [Online]. Available: https://all3dp.com/what-is-stl-file-format-extension-3d-printing/#pointnine. [Accessed: 15-Jun-2019].

[29] F. Committee, “Specification for Additive Manufacturing File Format (AMF) Version 1.2.” 2016.

[30] O. Rishi, “Feed Rate Effects In Freeform Filament Extrusion Feed Rate Effects

In Freeform Filament Extrusion," 2013.

[31] S. Crump, "'Apparatus for production of three-dimensional objects,'" 5.121.329, 1992.

[32] R. K. Enneti, S. J. Park, R. M. German, and S. V Atre, "Review : Thermal Debinding Process in Particulate Materials Processing," *Mater. Manuf. Process.*, vol. 27, no. 2, pp. 103–118, 2012.

[33] J. González-gutiérrez, G. B. Stringari, and I. Emri, "Powder Injection Molding of Metal and Ceramic Parts," in *Some Critical Issues for Injection Molding*, InTech, 2012, pp. 65–89.

[34] C. Kukla, J. Gonzalez-gutierrez, S. Cano, and S. Hampel, "Fused Filament Fabrication (FFF) of PIM Feedstocks," in *Proceedings of VI Congreso Nacional de Pulvimetalurgia y I Congreso Iberoamericano de Pulvimetalurgia*, 2017.

[35] A. Pajares and P. Miranda, "A simple graphite-based support material for robocasting of ceramic parts," *J. Eur. Ceram. Soc.*, 2017.

[36] K. Rane, "A comprehensive review of extrusion-based additive manufacturing processes for rapid production of metallic and ceramic parts," *Adv. Manuf.*, vol. 7, no. 2, pp. 155–173, 2019.

[37] S. Banerjee and C. J. Joens, "Debinding and sintering of metal injection molding (MIM) components," in *Handbook of Metal Injection Molding*, Woodhead Publishing Limited, 2012, pp. 133–180.

[38] R. I. Cable and T. K. Gupta, "Intermediate Stage Sintering," in *Sintering and related phenomena*, Gordon and Breach, 1967.

[39] A. Kumar, Y. Bai, A. Eklund, and C. B. Williams, "Effects of Hot Isostatic Pressing on Copper Parts Fabricated via Binder Jetting," *Procedia Manuf.*, vol. 10, pp. 935–944, 2017.

[40] M. N. Rahaman, "Kinetics and mechanisms of densification," in *Sintering of advanced materials*, Woodhead Publishing Limited, 2010, pp. 33–64.

[41] C. Kukla, J. Gonzalez-Gutierrez, C. Burkhardt, O. Weber, and C. Holzer, "The Production of Magnets by FFF-Fused Filament Fabrication," in *Proceedings of the Euro PM2017 Congress & Exhibition*, 2017, pp. 1–6.

[42] M. K. Agarwala, V. R. Jamalabad, N. A. Langrana, A. Safari, P. J. Whalen, and S. C. Danforth, "Structural quality of parts processed by fused deposition," *Rapid Prototyp. J.*, vol. 2, no. 4, pp. 4–19, 1996.

[43] M. Huang and H. Hsu, "Influence of injection moulding and sintering parameters on properties of 316L MIM compact," *Powder Metall.*, vol. 54, no. 3, pp. 299–307, 2013.

[44] J. Ryu, H. Kim, and H. T. Hahn, "Reactive Sintering of Copper Nanoparticles Using Intense Pulsed Light for Printed Electronics," *J. Eletronic Mater.*, vol. 40, no. 1, pp. 42–50, 2011.

[45] D. E. Dimla, M. Camilotto, and F. Miani, "Design and optimisation of conformal cooling channels in injection moulding tools," *J. Mater. Process. Technol.*, vol.

164–165, pp. 1294–1300, 2005.

[46] M. R. Clemente and M. R. O. Panão, “Introducing flow architecture in the design and optimization of mold inserts cooling systems,” *Int. J. Therm. Sci.*, vol. 127, pp. 288–293, 2018.

[47] A. Bejan and S. Lorente, *Design with constructal theory*. John Wiley & Sons, Inc., 2008.

[48] S. Lorente and A. Bejan, “Svelteness, freedom to morph, and constructal multi-scale flow structures,” *Int. J. Therm. Sci.*, vol. 44, pp. 1123–1130, 2005.

[49] S. A. Jahan, T. Wu, Y. Zhang, J. Zhang, A. Tovar, and H. Elmounayri, “Thermo-mechanical design optimization of conformal cooling channels using design of experiments approach,” *Procedia Manuf.*, vol. 10, pp. 898–911, 2017.

[50] M. Mazur, P. Brincat, M. Leary, and M. Brandt, “Numerical and experimental evaluation of a conformally cooled H13 steel injection mould manufactured with selective laser melting,” *Int. J. Adv. Manuf. Technol.*, vol. 93, no. 1–4, pp. 881–900, 2017.

[51] T. Wu, S. A. Jahan, Y. Zhang, J. Zhang, and H. Elmounayri, “Design optimization of plastic injection tooling for additive manufacturing,” *Procedia Manuf.*, vol. 10, pp. 923–934, 2017.

[52] T. J. J. Ferreira, “Microinjection moulding of austenitic stainless steel reinforced with carbon nanotubes,” University of Coimbra, 2017.

[53] F. Barreiros, “Optimização da moldação por injecção de pós de resíduos industriais inorgânicos,” University of Coimbra, 2002.

[54] T. J. Ferreira and M. T. Vieira, “Optimization of MWCNT – Metal Matrix Composites feedstocks,” *Ciência Tecnol. dos Mater.*, vol. 29, no. 1, pp. e87–e91, 2017.

[55] M. Sahli and J. Gelin, “Development of a feedstock formulation based on polypropylene for micro-powder soft embossing process of 316L stainless steel micro-channel part,” *Int. J. Adv. Manuf. Technol.*, vol. 69, no. 9–12, pp. 2139–2148, 2013.

[56] M. E. Sotomayor, A. Várez, and B. Levenfeld, “In fl uence of powder particle size distribution on rheological properties of 316 L powder injection moulding feedstocks,” *Powder Technol.*, vol. 200, no. 1–2, pp. 30–36, 2010.

[57] F. M. Barreiros and M.-T. F. Vieira, “Fine tuning injection feedstock by nano coating SS powder,” *Met. Powder Rep.*, vol. 64, no. 9, pp. 18–21, 2009.

[58] E. W. De Sequeiros, “Microfabricação de Componentes Metálicos por Microgravação,” Universidade do Porto, 2014.

[59] K. Harika, T. Likhitha, P. V. Rani, and R. Ramakanth, “Experimental Determination and Comparison of Heat Transfer Coefficient and Pressure Drop for Water and Copper Oxide Nano Fluid in Shell and Tube Heat Exchangers using Helical Baffles,” no. July, 2017.

[60] M. Stevenson, “3D Printer Metal Filament – 2018 Market Overview,” 2018. [Online]. Available: https://all3dp.com/2/3d-printer-metal-filaments-2018-

market-overview/. [Accessed: 16-Jun-2019].

[61] Y. Lin and K. Hwang, “Swelling of Copper Powders during Sintering of Heat Pipes in Hydrogen-Containing Atmospheres,” vol. 51, no. 12, pp. 2251–2258, 2010.

[62] D. F. Heaney, “Vacuum sintering,” in *Sintering of advanced materials*, 2010, pp. 189–221.

[63] NADCA, “section 4 A,” in *NADCA Product Specification Standards for Die Castings*, 2009, pp. 1–44.

[64] C. Edge and M. Solutions, “Flatness Tolerances, Technical Resources— Perforated Metal Standards.” .

[65] K. Diao and Y. Zhao, “Heat transfer performance of sintered Cu microchannels produced by a novel method,” *Int. J. Heat Mass Transf.*, vol. 139, pp. 537–547, 2019.

[66] L. Ren *et al.*, “Process Parameter Optimization of Extrusion-Based 3D Metal Printing Utilizing PW – LDPE – SA Binder System,” *Materials (Basel).*, vol. 10, no. 3, 2017.

[67] D. Wang, Y. Liu, Y. Yang, and D. Xiao, “Theoretical and experimental study on surface roughness of 316L stainless steel metal parts obtained through selective laser melting,” *Rapid Prototyp. J.*, vol. 22, no. 4, pp. 706–716, 2016.

APPENDIX A

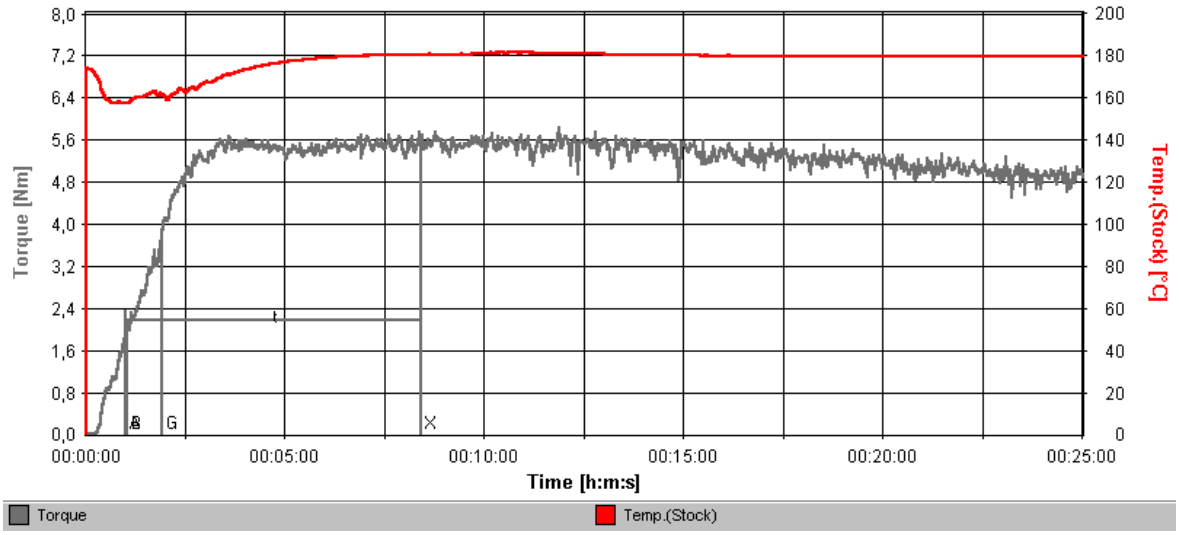

Figure 32 – Torque of feedstock with 60:40 vol.% of M1 binder and other additives function of mixing time

APPENDIX B

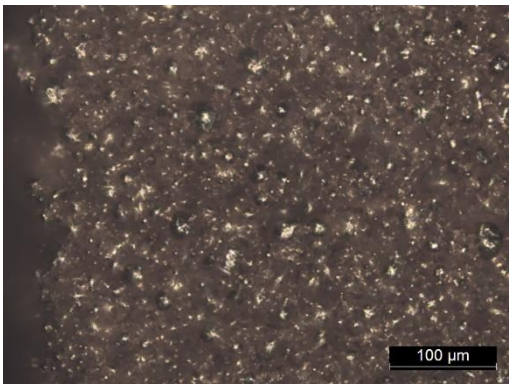

Figure 33 - Insert tip topography (200x)

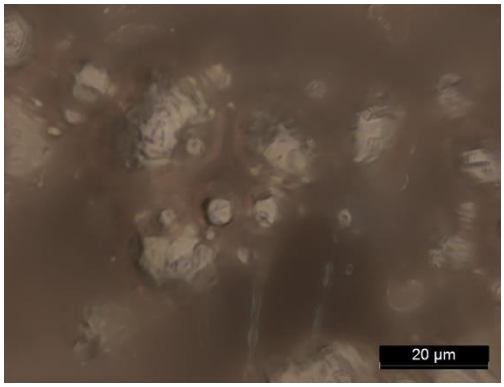

Figure 34 - Insert tip topography (1000x)

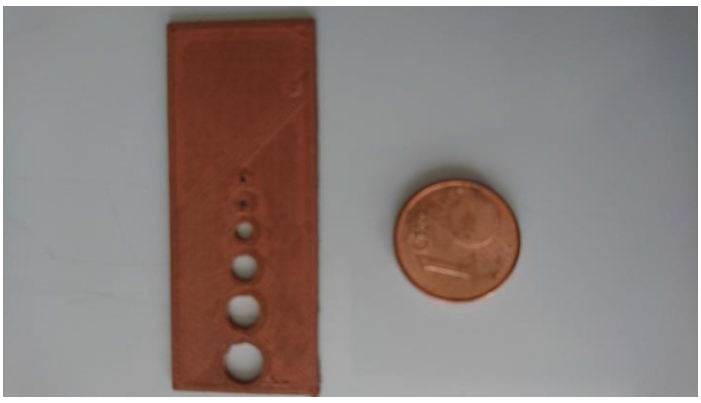

Figure 35 - Several holes with different diameters

Figure 36 - Copper filament for FDMet

Figure 37 - View of a FDMet produced copper part with a conformal channel

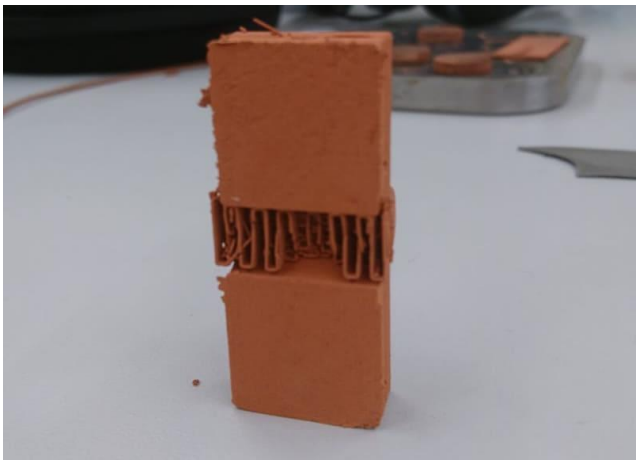

Figure 38 - View of a FDMet produced copper part with a conformal channel

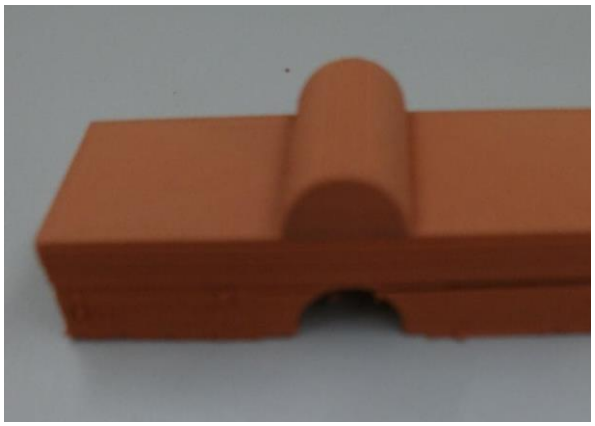

Figure 39 - View of a FDMet produced copper part with a conformal channel

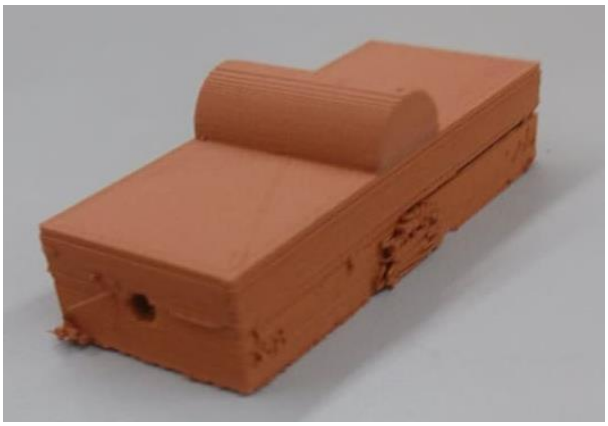

Figure 40 - View of a FDMet produced copper part with a conformal channel

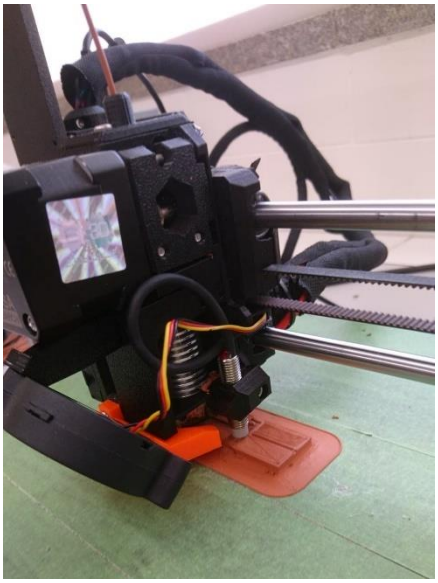

Figure 41 - Printing a copper part with a conformal channel by FDMet

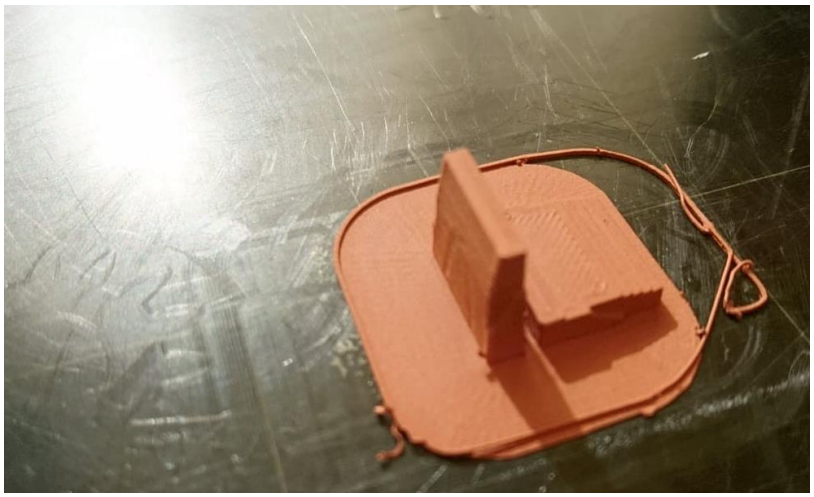

Figure 42 - FDMet produced vertical and horizontal insert tips with conformal channel

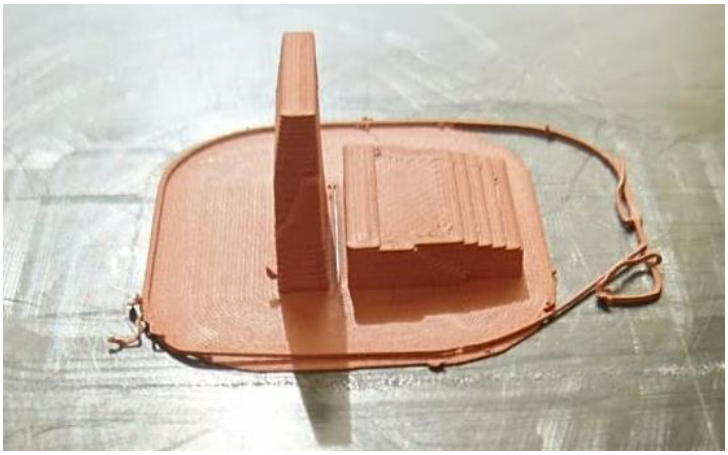

Figure 43 - FDMet produced vertical and horizontal insert tips with conformal channel

Figure 44 - Section of FDMet produced copper insert with conformal channels

Figure 45 - Bottom view of FDMet produced copper part with complex geometry

Figure 46 - Upper view of FDMet produced copper part with complex geometry

Figure 47 - FDMet produced copper parts with complex geometry

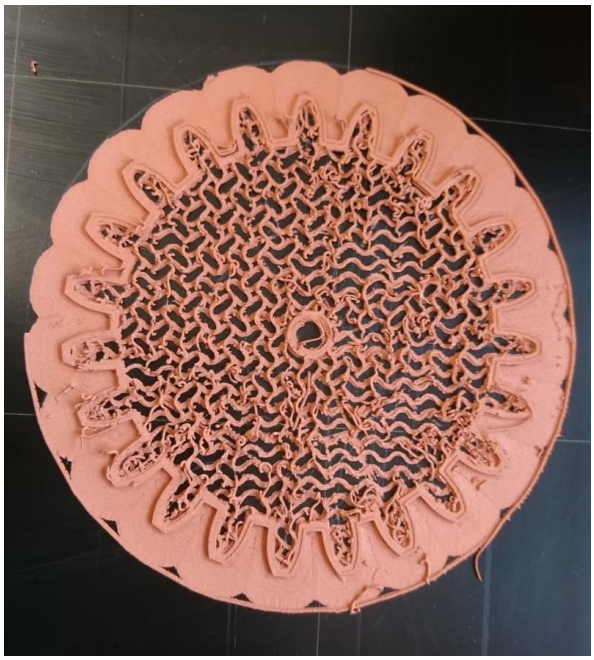

Figure 48 - FDMet produced copper helicoidal gear with 20% infill

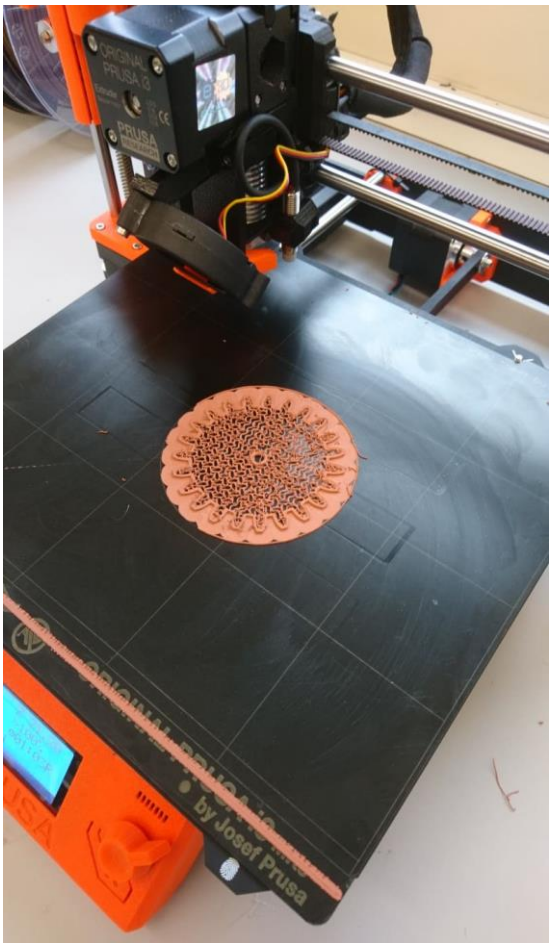

Figure 49 - Printing by FDMet a copper helicoidal gear with 20% infill